Received: 23 January 2026 | Accepted: 24 April 2026

DOI: 10.1111/syen.70051

ORIGINAL ARTICLE

Systematic Entomology | Royal Entomological Society

Genomic-based species delimitation reveals cryptic diversity and semi-permeable species boundaries in a *Chorthippus* (Orthoptera: Acrididae) grasshopper complex from Greece

Marina Trillo | **Joaquín Ortego**

Department of Ecology and Evolution, Estación Biológica de Doñana, EBD-CSIC, Seville, Spain

Correspondence
Marina Trillo and Joaquín Ortego, Department of Ecology and Evolution, Estación Biológica de Doñana, EBD-CSIC, Avda. Américo Vespucio 26, E-41092 Seville, Spain.
Email: marina.trillo@ebd.csic.es and joaquin.ortego@csic.es

Funding information
Ministerio de Ciencia e Innovación, MCIN/AEI/10.13039/501100011033, Grant/Award Number: TED2021-129328B-I00; European Union NextGenerationEU/PRTR, Grant/Award Number: TED2021-129328B-I00; Ministerio de Ciencia e Innovación and European Regional Development Fund, MCIN/AEI/10.13039/501100011033/FEDER, UE, Grant/Award Number: PID2021-123298NB-I00

Editor: Gael J. Kergoat

Abstract

Recent Pleistocene radiations often generate cryptic diversity and semi-permeable species boundaries, challenging species delimitation and the reconstruction of evolutionary histories. Here, we investigate these processes in a species complex of *Chorthippus* grasshoppers from Greece using genome-wide ddRAD-seq data combined with geometric morphometrics. Phylogenomic analyses indicate that diversification occurred during the Middle Pleistocene and identify two major geographic clades separated by the Corinthian Gulf, followed by finer-scale divergence within the Peloponnese Peninsula. Most taxa form well-supported, reciprocally monophyletic lineages despite recent divergence, although several populations at range margins show signatures of historical hybridization, revealing semi-permeable species boundaries shaped by secondary contact. Introgression is geographically restricted and strongly asymmetric, occurring primarily from long-winged into short-winged taxa, consistent with differences in dispersal capacity. Species delimitation analyses largely support current taxonomy but also identify three previously unrecognized evolutionary lineages corresponding to geographically restricted populations, uncovering additional cryptic diversity. Morphological analyses reveal pronounced stasis in shape-related traits across lineages, with wing length emerging as the main axis of differentiation. Phylogenetic reconstructions indicate multiple independent reductions in wing size, highlighting repeated evolutionary transitions toward reduced dispersal. In at least one lineage, a pronounced geographic cline in wing length is mirrored by shallow phylogenetic structure, supporting an incipient evolutionary shift in dispersal capacity rather than phenotypic plasticity. Admixed populations consistently retain short-winged phenotypes, suggesting strong selection on dispersal-related traits despite genomic introgression. Overall, our results demonstrate how topographic complexity, Pleistocene climatic oscillations and dispersal-related morphology interact to shape diversification and maintain lineage integrity in a Mediterranean biodiversity hotspot.

KEYWORDS
Chorthippus, ddRAD-seq, geometric morphometrics, hybrid zones, narrow endemic species, species complex, species delimitation

INTRODUCTION

Cryptic species and semi-permeable species boundaries are increasingly recognized as pervasive outcomes of recent diversification (Bickford et al., 2007; Seehausen, 2004). In some cases, genetic discontinuities may be sharp despite minimal phenotypic divergence, whereas in others, secondary contact and different levels of introgression can blur taxonomic limits and challenge species delimitation (Barton & Hewitt, 1985; Harrison & Larson, 2014). This is often the case in species complexes that originated during the Pleistocene, where morphology evolves under strong functional constraints and reproductive isolation is often incomplete (e.g., Ortego & Knowles, 2022). A major factor contributing to the emergence of such complex evolutionary scenarios has been the climatic oscillations of the Quaternary, which profoundly shaped the spatial distribution and genetic composition of temperate biotas (Hewitt, 1996, 2000). These cycles recurrently fragmented populations through contractions into glacial or interglacial refugia (Bennett & Provan, 2008; Carstens & Knowles, 2007), igniting genetic differentiation and exposing populations to distinct selective regimes in isolation, thereby promoting divergence and speciation (Stewart et al., 2010). Conversely, range expansions and elevational or latitudinal shifts repeatedly brought lineages into secondary contact, providing opportunities for gene flow (Knowles & Massatti, 2017; Maier et al., 2019; Tonzo & Ortego, 2021). If reproductive barriers among incipiently diverging lineages are weak, secondary contact can lead to introgressive hybridization, lineage fusion, or even speciation reversal (Mallet et al., 2016; Nevado et al., 2018). Hence, Pleistocene climate dynamics are hypothesized to have acted both as 'species pumps' and 'melting pots', contributing to divergence and gene flow across different stages along the speciation continuum (April et al., 2013; Ebdon et al., 2021; Haffer, 1969; Hewitt, 2000). As a result, phylogenetic relationships in complexes of recently diverged taxa are often obscured by both incomplete lineage sorting (Maddison & Knowles, 2006) and reticulate evolution, challenging species delimitation and the reconstruction of evolutionary histories (Degnan & Rosenberg, 2009; Payseur & Rieseberg, 2016). Elucidating how lineages persist and diversify under these conditions, an issue central to evolutionary biology (Coyne & Orr, 2004; Nosil, 2008), requires integrative frameworks that combine genomic, phenotypic and ecological data.

Orthopterans include numerous species complexes in which recent divergence, hybridization and limited phenotypic differentiation contribute to substantial taxonomic uncertainty, making them particularly suitable model systems for testing complex scenarios of species delimitation and for investigating the evolutionary, ecological and geological processes underlying species formation (e.g., Hawlitschek et al., 2022; Huang et al., 2020; Le Flanchec et al., 2026; Ortego & Noguerales, 2025; Schmidt et al., 2024). The limited dispersal ability of most orthopterans and their ecological specialization often promote strong population subdivision (Chapco & Litzenberger, 2002; Mason et al., 1995), while acoustic and morphological traits offer different axes of differentiation (Neumeister et al., 2025; Noguerales et al., 2018; Vedenina et al., 2024; Willemse et al., 2009). However, within complexes of closely related species, most morphological traits exhibit strong stasis, with variation in wing development representing a notable exception. Wing polymorphism and polyphenism, together with frequent evolutionary transitions toward reduced dispersal capacity (e.g., from macropterism to brachypterism) (Harrison, 1980; Roff, 1990, 1994; Zera & Denno, 1997), have repeatedly contributed to taxonomic uncertainty within Orthoptera (e.g., Ortego et al., 2021). As in many other organisms, wing-size reduction and transitions to flightlessness are particularly frequent in taxa inhabiting insular systems and montane-alpine environments (Ikeda et al., 2012; Wright et al., 2016). Such differences in dispersal capacity have important microevolutionary and demographic consequences and have been linked to contrasting rates of geographical diversification (Ortego et al., 2021; Suárez et al., 2022), asymmetric introgression (Dussex et al., 2016; Ortego et al., 2021; Ortego & Knowles, 2022) and range expansions (Hochkirch & Damerau, 2009). Altogether, this combination of pronounced genetic structure, low vagility and otherwise conservative morphologies makes recent radiations of grasshoppers excellent model systems for studying cryptic speciation and semi-permeable species boundaries, and for elucidating the mechanisms driving the speciation process.

Here, we focus on a complex of grasshoppers of the genus *Chorthippus* Fieber (Orthoptera: Acrididae) distributed in southern Greece, which comprises several allopatric taxa with limited phenotypic differentiation and represents a challenging case of recent diversification. This complex encompasses a mosaic of microendemic lineages with highly restricted ranges, including one Ionian island-endemic *C. sangiorgii* (Finot) and three taxa with adjacent allopatric distributions in the southern Peloponnese Peninsula—*C. moreanus* Willemse, Helversen & Odé, *C. parnon* Willemse, Helversen & Odé, and *C. crassiceps* (Ramme). Only one putative species, *C. pulloides* Ramme, exhibits a broader distribution, from the Pindus Mountains to the Peloponnese, where many populations occur in close proximity to the other three taxa present in the region. Although some studies have emphasized the acoustic distinctiveness of the different putative species, all taxa show pronounced morphological similarity, aside from differences among taxa and certain populations in the degree of forewing development (Ramme, 1926, 1927; Willemse, 1984, 1985, 1986; Willemse et al., 2009). Accordingly, several populations remain difficult to classify because they display intermediate or atypical phenotypes (Willemse et al., 2009), suggesting a history of hybridization and introgression (e.g., Ortego et al., 2026). The fact that several narrow-range endemics within this complex are currently listed as 'Near Threatened' on the IUCN Red List (Hochkirch et al., 2016) underscores the conservation relevance of clarifying their evolutionary independence. Altogether, this combination of restricted ranges and largely allopatric distributions, together with subtle morphological and ecological differentiation, exemplifies the longstanding difficulty of testing taxonomic hypotheses when reproductive isolation among candidate species cannot be assessed in contact zones (Coyne & Orr, 2004; Mayr, 1963). Under this scenario, comprehensive taxonomic and population sampling, combined with integrative analyses of

genomic and morphological data, can provide critical insights into the extent of reproductive isolation and evolutionary independence of putative taxa, and offer a robust baseline for species delimitation (Coyne & Orr, 1989; Dynesius & Jansson, 2014).

In this study, we integrate fine-scale population sampling, genome-wide data (ddRAD-seq) and geometric and linear morphometric analyses to delimit species and investigate patterns of post-divergence gene flow within the focal complex. Specifically, we address three main objectives and their associated hypotheses. First, (i) we reconstruct phylogenetic relationships and assess species boundaries under both the phylogenetic and genotypic cluster species concepts (De Queiroz, 2007), testing the hypothesis that narrowly distributed, allopatric taxa represent evolutionarily independent lineages despite limited morphological differentiation. We predict that genomic data will recover well-supported lineages corresponding to described taxa, while also revealing cases of shallow divergence or admixture that obscure phylogenetic resolution. Second, (ii) we apply coalescent-based demographic modelling to evaluate the extent, direction and timing of secondary contact and introgression in populations identified as admixed in clustering analyses, testing the hypothesis that Pleistocene-driven range shifts promoted recurrent episodes of secondary contact among partially isolated lineages, resulting in geographically restricted processes of lineage fusion. Finally, we (iii) integrate genomic and morphometric analyses to assess congruence across independent data sources in delimiting species boundaries, to test whether transitions to brachypterism have occurred multiple times throughout the evolutionary history of the complex, and to evaluate the extent to which hybridization has contributed to phenotypic variation. We hypothesize that wing reduction and reduced dispersal capacity have evolved multiple times in association with population subdivision and habitat patch isolation (Harrison, 1980; Roff, 1990, 1994), and that introgression has locally shaped morphological variation without fully eroding species boundaries. By combining genomic and morphological data with species delimitation and demographic inference, our study provides a refined and integrative framework for disentangling recent diversification with gene flow and for understanding the proximate processes triggering diversification within the Mediterranean biodiversity hotspot (Myers et al., 2000).

MATERIALS AND METHODS

Taxonomic and population sampling

During the summers of 2021 and 2023, we sampled 34 populations that cover the entire range of all taxa within the species complex of the genus *Chorthippus* from central and southern Greece, with a specific focus on the Peloponnese region (Table 1). This complex includes the mainland taxa *C. pulloides*, *C. moreanus*, *C. parnon* and *C. crassiceps*, as well as the Ionian island-endemic *C. sangiorgii*. While *C. pulloides* and *C. sangiorgii* are short-winged, typical forms of *C. moreanus*, *C. parnon* and *C. crassiceps* are long-winged, with forewings that reach or surpass the hind knee (Willemse et al., 2009). Sampling was designed to maximize coverage of the geographic and phenotypic variation of the complex and included populations of uncertain taxonomic status (Willemse et al., 2009). We aimed to collect at least eight adult individuals per population. However, in some localities, only a few adult males—or mostly nymphs—were found during sampling. Because wings are not fully developed in immature individuals, these limitations affected only the morphometric analyses. For genomic analyses, we ensured a minimum sample size of eight individuals per population, including nymphs when necessary (Table 1). Spatial coordinates were recorded using a Global Positioning System (GPS), and whole specimens were preserved at −20°C in 1500 μL of 100% ethanol until needed for genomic and morphometric analyses. All samples were obtained under permits granted by the Greek Ministry of the Environment and Energy (permit nos. YPEN/DDD/34736/1134 and YPEN/DDD/32363/1054). Further details on sampled taxa and populations are provided in Table 1.

Genomic library preparation and genomic data processing

We extracted and purified DNA from each specimen using NucleoSpin Tissue kits (Macherey-Nagel, Düren, Germany). We processed DNA into different genomic libraries using the double-digestion restriction-fragment-based procedure (ddRAD-seq) described in Peterson et al. (2012) and detailed in Methods S1. Raw sequences were demultiplexed and preprocessed using STACKS v. 2.66 (Rochette et al., 2019) and assembled using IPYRAD v. 0.9.93 (Eaton & Overcast, 2020). Methods S2 provides all details on sequence data filtering and assembling.

Phylogenomic inference

We reconstructed the phylogenetic relationships among populations of the studied complex using two independent analytical approaches: the maximum-likelihood (ML) method implemented in RAXML v. 8.2.12 (Stamatakis, 2014) and the multi-species coalescent-based approach implemented in BPP v. 4.7.0 (analysis A01; Flouri et al., 2018). To avoid the confounding effects of hybridization on phylogenetic inference and species delimitation (Chan et al., 2023; see Species delimitation analyses), we excluded from the analyses admixed populations identified by Bayesian clustering analyses in STRUCTURE (see Population genetic structure and admixture and Population genetic structure). To reduce computational demands, we only included a single representative individual per population—the one with the lowest proportion of missing data—for phylogenomic analyses.

raxml

We ran RAXML using a matrix of concatenated SNPs (all SNPs per locus; *.snp* file from IPYRAD) edited in the R v. 4.4.0 (R Core Team, 2021)

TABLE 1 Geographical location of studied populations of the *Chorthippus* species complex in Greece, including their taxonomic status before (putative species) and after (delineated species) species delimitation with DELINEATE (see Species delimitation analyses) and genetic admixture (Population genetic structure) analyses.

Putative species	Delineated species	Population	Code	Latitude	Longitude	Elevation	*n* (gen.)	*n* (morp.)
C. sangiorgii	*C. sangiorgii*	Lefkada Island—Marantochori	MARA	38.638862	20.675340	200	8	4
	C. sangiorgii	Cephalonia Island—Chavdata[a]	CHAV	38.194927	20.372910	190	8	5
C. pulloides	DelineatedSp001	Mt. Kakarditsa	KAKA	39.544839	21.18708	1860	8	5
	DelineatedSp002	Mt. Akarnanika	AKAR	38.834396	20.982888	910	8	3
	C. pulloides	Mt. Panachaiko	PANA	38.207062	21.868688	1730	8	5
	C. pulloides	Agia Triada	TRIA	37.847903	21.653582	490	8	5
	C. pulloides	Mt. Erymanthos	ERYM	37.951604	21.793806	1990	8	5
	C. pulloides	Metochi	METO	38.003929	21.934568	880	8	5
	C. pulloides	Mt. Chelmos[a]	CHEL	37.975511	22.202851	2260	10	5
	C. pulloides	Mt. Kyllini	KYLL	37.939056	22.396115	2350	8	5
	Hybrid	Mt. Maenalon	MAEN	37.644274	22.276261	1840	8	5
	Hybrid	Krioneri	KRIO	37.576332	22.551306	830	7	2
	Hybrid	Agios Petros	PETR	37.332440	22.557441	880	8	5
	Hybrid	Mt. Parnon	PARN	37.281016	22.612383	1870	8	5
	Hybrid	Mt. Taygetus—Portes	TAYP	36.957716	22.351548	2240	8	5
C. moreanus	*C. moreanus*	Stemnitsa	STEM	37.535469	22.089126	1050	8	1
	C. moreanus	Bassae[a]	BASS	37.429405	21.899759	1120	10	5
	C. moreanus	Pylos	PYLO	36.884127	21.696716	450	8	4
	C. moreanus	Nedousa	NEDO	37.134629	22.229493	920	8	5
	Hybrid	Taygetus—EOS Katafygio	TAYK	36.950079	22.367255	1560	8	5
	C. moreanus	Cape Tenaro	TENA	36.400436	22.485514	10	8	5
	Hybrid	Polidroso	POLI	37.141440	22.613072	1030	8	5
C. parnon	*C. parnon*	Kremasti[a]	KREM	36.959406	22.870150	790	8	5
	C. parnon	Argeiteika	ARGE	36.614777	23.002187	460	10	5
	C. parnon	Cape Maleas	MALE	36.438923	23.173909	60	8	5
	DelineatedSp003	Kythira Island—Potamos	POTA	36.304524	22.976823	310	8	5
C. crassiceps	*C. crassiceps*	Sofiko	SOFI	37.800653	23.038608	440	8	5
	C. crassiceps	Arachneo	ARAC	37.66534	22.930611	650	8	6
	C. crassiceps	Palaia Epidavros	EPID	37.647412	23.154687	130	8	4
	C. crassiceps	Methana[a]	METH	37.627264	23.370095	310	8	5
	C. crassiceps	Mt. Didymo	DIDY	37.477009	23.220686	1040	10	5

Note: Hybrid populations were not included in species delimitation analyses (see Phylogenomic inference). [a]Type localities or the sampling sites geographically closest to the respective type localities of each taxon. *n* (gen.) = number of genotyped individuals; *n* (morp.) = number of individuals used for geometric morphometric analyses.

package 'phrynomics' (B. Banbury, http://github.com/bbanbury/phrynomics). Five individuals of *C. willemsei* Harz, a species belonging to the same subgenus (*Glypthobothrus*) as the focal species complex (Cigliano et al., 2025), were used as an outgroup in RAXML analyses. The input dataset contained 15,455 SNPs. We applied an ascertainment bias correction using the conditional likelihood method (Lewis, 2001), used a GTR-GAMMA model of nucleotide evolution, performed 100 rapid bootstrap replicates, and searched for the best-scoring maximum likelihood tree. To explore the phylogenetic placement of admixed populations, we performed an additional RAXML analysis on a dataset (19,661 SNPs) including all sampled populations (i.e., without excluding admixed populations).

bpp

We used whole ddRAD-seq loci (*.loci* file from IPYRAD) to run tree estimation A01 analyses in BPP (Flouri et al., 2018). The *.loci* file from ipyrad was edited and converted into a BPP input file using a custom R script (J. Ortego, https://github.com/OrtegoLab/ipyrad2bpp). As BPP analyses are computationally highly demanding, we limited the dataset to 1000 loci. We set uniform rooted trees as species tree prior, applied an automatic adjustment of fine-tune parameters, set the diploid option to indicate that the input sequences are unphased, and adjusted the inverse-gamma distributions of θ ($\alpha = 3, \beta = 0.04$) and τ ($\alpha = 3, \beta = 0.07$) priors according to empirical estimates calculated based on the number of

segregating sites per site (Huang et al., 2020). Note that BPP analyses do not require defining an outgroup, as the program samples the root position along with the other nodes of the tree. We ran two independent replicate analyses for 400,000 generations, sampling every 2 generations, after a burn-in of 20,000 generations.

Estimation of divergence time

Phylogenetic trees inferred using RAXML and BPP (see Phylogenomic inference) were fitted as the fixed topology in A00 analyses in BPP to estimate the posterior distribution of divergence times (τ; Rannala & Yang, 2003; Flouri et al., 2018) among populations. We ran the analyses using the same dataset and settings considered for tree inference A01 analyses in BPP described in Phylogenomic inference section. In order to ensure the convergence of the runs (ESS > 200), we ran two independent replicate analyses for 2,000,000 generations, sampling every 2 generations, after a burn-in of 100,000 generations. We estimated divergence times using the equation $\tau = 2\mu t$, where τ is the divergence in substitutions per site estimated by BPP, μ is the per site mutation rate per generation, and t is the absolute divergence time in years (Walsh, 2001). We considered the mutation rate per site per generation of 2.8×10^{-9} estimated for *Drosophila melanogaster* (Keightley et al., 2014), which is similar to the spontaneous mutation rate estimated for the butterfly *Heliconius melpomene* (2.9×10^{-9}; Keightley et al., 2015).

Species delimitation analyses

We performed constrained, partitioned species delimitation analyses using the program DELINEATE v. 1.2.3, an approach that incorporates an explicit model of protracted speciation within the multipopulation coalescent framework to identify sets of lineages representing distinct species (Sukumaran et al., 2021). Based on a population-level ultrametric phylogeny and prior knowledge of species assignment for a subset of populations in the dataset, DELINEATE estimates whether the remaining populations belong to an already described species or represent distinct evolutionary lineages consistent with a separate species (Sukumaran et al., 2021). We ran DELINEATE analyses using ultrametric trees obtained from A00 analyses in BPP (see Estimation of divergence time), considering the slightly different topologies inferred using RAXML and analysis A01 in BPP (see Phylogenomic inference and Phylogenomic inference and divergence time estimation), and a species assignment reference file indicating whether each population corresponded to a known nominal species (status = 1) or to an unknown species identity (status = 0). We made status assignments considering nomenclatural priority and the current taxonomic understanding of the group, in conjunction with the evolutionary relationships among population lineages inferred from the phylogeny (Sukumaran et al., 2021). Specifically, we assigned populations to a known or unknown nominal species status based on the taxonomic literature and information on species distributions available at Orthoptera Species File (https://orthoptera.speciesfile.org/; Cigliano et al., 2025; Willemse et al., 2009; see Table 1). Two populations assigned in the literature to *C. pulloides* (KAKA and AKAR, from central Greece) and one population assigned to *C. parnon* (POTA, from Kythira Island) did not cluster monophyletically within the clade including the type locality of their respective putative species and were therefore treated as having an unknown species identity in DELINEATE analyses (Table 1). Likewise, two populations assigned in the literature to *C. crassiceps* (SOFI and ARAC) were also treated as having an unknown species identity, as they formed a well-supported, distinct clade and exhibited significantly shorter forewings than the clade including the type locality of the species (see Phylogenomic inference and divergence time estimation; Table 1).

Testing for introgression

We used four-taxon ABBA/BABA tests based on the *D*-statistic to evaluate whether the different populations of a given taxon have experienced genetic introgression from other taxa (Durand et al., 2011). Assuming that the sister taxa P1 and P2 diverged from P3 and an outgroup species O, the *D*-statistic is used to test the null hypothesis of no introgression ($D = 0$) between P3 and P1 or P2. *D*-values significantly different from zero indicate gene flow between P1 and P3 ($D < 0$) or between P2 and P3 ($D > 0$). Tests were designed to evaluate introgression from one taxon (P3) into each population of another taxon (P1). To this end, for both P2 and P3 we used reference populations with no signatures of genetic introgression from other taxa based on Bayesian clustering analyses in STRUCTURE and inferences from exhaustive *D*-statistic tests. The highly divergent lineage from Mt. Kakarditsa (KAKA; Figure 2) was used as the outgroup (P4) in all analyses. *D*-statistic tests were exclusively focused on comparisons involving *C. pulloides*, *C. moreanus* and *C. parnon* and pairs of taxa with adjacent or partially overlapping distributional ranges. We did not include *C. crassiceps* in these analyses because neither STRUCTURE nor exploratory *D*-statistic tests provided evidence that this taxon was involved in genetic admixture or introgression with other taxa (Population genetic structure). *D*-statistic tests were run as implemented in the IPYRAD pipeline (Eaton & Overcast, 2020).

Population genetic structure and admixture

We used the Bayesian Markov chain Monte Carlo clustering method implemented in the program STRUCTURE v. 2.3.3 (Pritchard et al., 2000) to quantify genetic structure and admixture across populations of the four putative species distributed in the Peloponnese Peninsula (*C. pulloides*, *C. moreanus*, *C. parnon* and *C. crassiceps*; Table 1), where taxa present adjacent distributions and may hybridize in contemporary and/or historical contact zones. We ran STRUCTURE analyses with 200,000 MCMC iterations following a burn-in of 100,000 iterations, assuming correlated allele frequencies and an admixture model, and without using prior population information. We conducted 15 independent runs for each value of the number of genetic clusters (*K*),

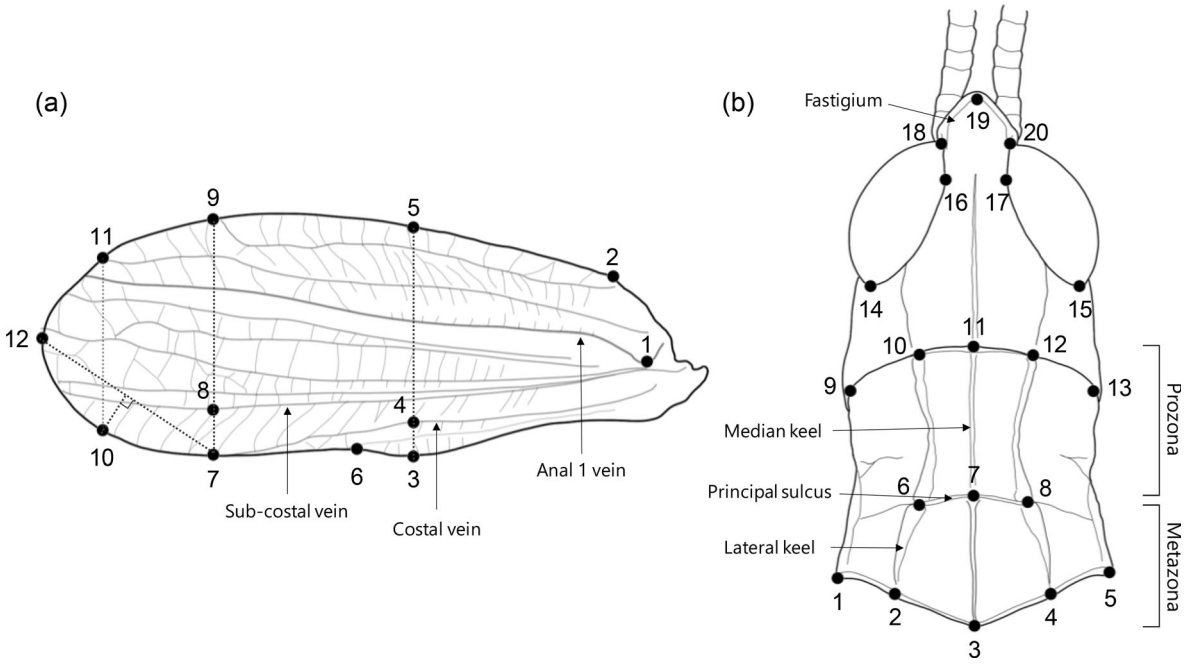

FIGURE 1 Landmarks used to characterize (a) forewing and (b) pronotum-head combined in males of studied populations of the *Chorthippus* species complex in Greece. A full description of landmarks is provided in Table S1. Illustrations by Marina Trillo.

with *K* ranging from 1 to 8, to estimate the most likely number of genetic clusters. We retained the 10 runs having the highest likelihood for each value of *K*. As recommended by Gilbert et al. (2012) and Janes et al. (2017), we used two complementary statistics to determine the value of *K* that best describes the data: the log probabilities of the data (LnPr(X|*K*); Pritchard et al., 2000) and Δ*K* (Evanno et al., 2005), calculated as implemented in STRUCTURE HARVESTER (Earl & vonHoldt, 2012). We used CLUMPP v. 1.1.2 with the Greedy algorithm to align replicate runs of STRUCTURE for the same *K* value (Jakobsson & Rosenberg, 2007), and DISTRUCT v. 1.1 (Rosenberg, 2004) to visualize the individuals' probabilities of population membership in bar plots.

Timing of divergence and admixture

Bayesian clustering analyses in STRUCTURE revealed that several populations from the Peloponnese Peninsula present a high proportion of admixed ancestry and *D*-statistic tests confirmed that they originated from historical hybridization between *C. pulloides* and *C. moreanus* (MAEN and TAYP), between *C. pulloides* and *C. parnon* (KRIO, PETR and PARN), or between *C. moreanus* and *C. parnon* (POLI) (for details, see the Results section). We used the coalescent-based approach implemented in FASTSIMCOAL2 (Excoffier et al., 2021) to infer demographic parameters describing the secondary contact event that led to the formation of these admixed populations, including timing of admixture and the proportion of ancestry contributed by each parental species. Due to computational constraints, we focused the demographic analyses on a subset of three admixed populations (MAEN, PARN and TAYP). We focused on models assuming initial divergence in isolation followed by secondary contact, as this is the most parsimonious scenario given the allopatric distributions of the focal taxa and their recent divergence (<0.5 Ma) (see the Results section). This approach avoids the inherent difficulty in distinguishing between early gene flow and incomplete lineage sorting in such young lineages. Furthermore, our models did not constrain the timing of the admixture event, allowing for the inference of gene flow at any point following the initial divergence.

We first tested two alternative demographic models of divergence and admixture and then estimated demographic parameters and their respective 95% confidence intervals under the best-supported model. The two models considered included scenarios of (i) divergence in strict isolation followed by an admixture event and the absence of contemporary gene flow (Model A), and (ii) divergence in strict isolation followed by an admixture event with ongoing gene flow (Model B) (Figure S1). Each analysis included one admixed population (MAEN, PARN, or TAYP) and one representative non-admixed population from each of the respective parental taxa. Parental demes were selected from non-admixed (i.e., putatively pure) populations assigned to the same genetic clusters as the focal admixed population (see Population genetic structure and Figure 3), resulting in the three population triplets: KYLL-MAEN-PYLO, KYLL-PARN-MALE and KYLL-TAYP-TENA. Further details on FASTSIMCOAL2 analyses and model selection are provided in Methods S3.

Morphometric analyses

We applied both geometric and linear morphometric approaches to characterize variation in the forewing (tegmen) and the combined

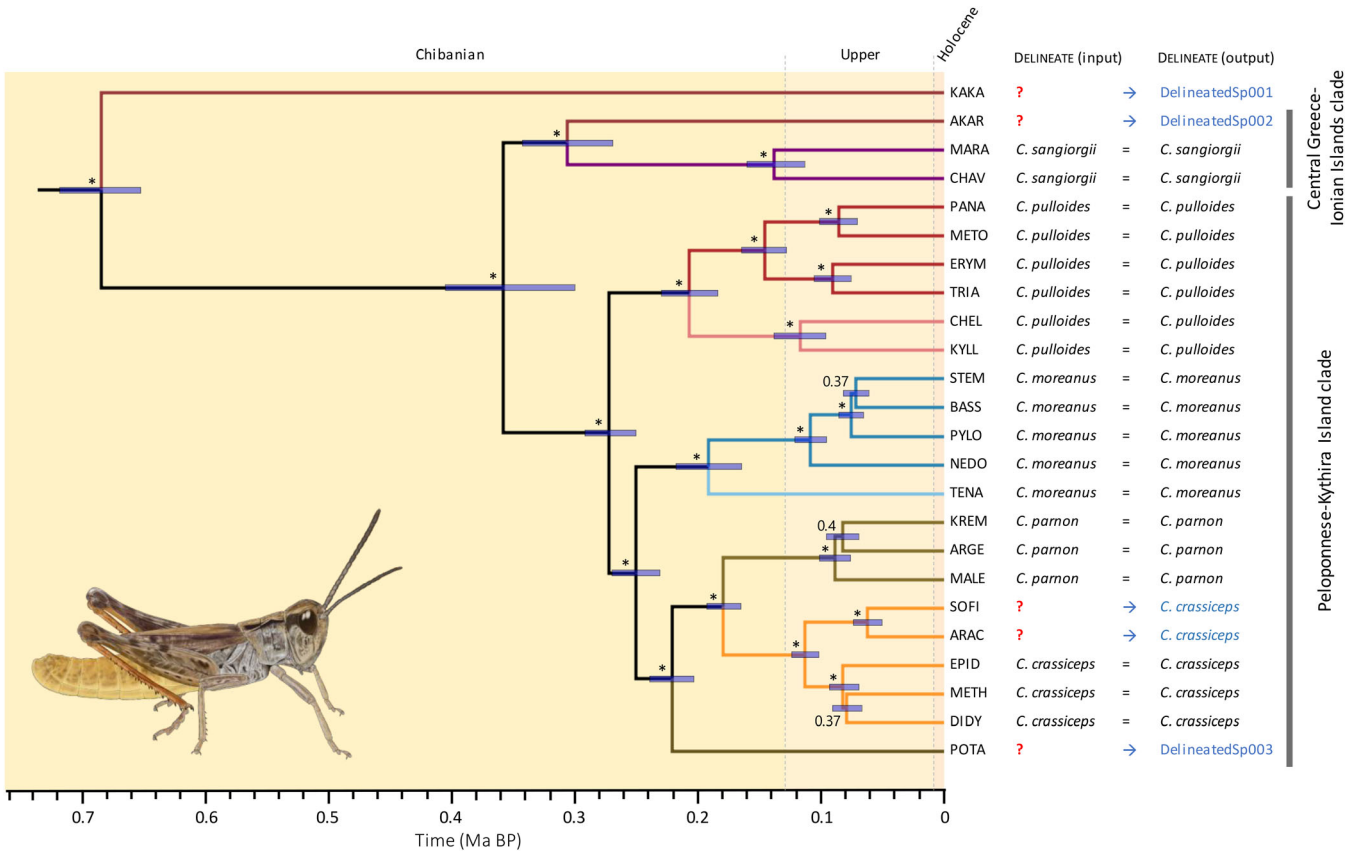

FIGURE 2 Phylogenetic tree and divergence times estimated using BPP (analyses A01 and A00, respectively) for the analyzed populations of the *Chorthippus* species complex in Greece. Admixed populations identified by STRUCTURE for $K = 6$ (marked with an asterisk in Figure 3b) were excluded from phylogenomic analyses (see Testing for introgression and Population genetic structure). Bayesian posterior probabilities estimated with BPP are indicated at nodes (* > 0.95). Bars on nodes indicate 95% highest posterior densities (HPD) of divergence times, estimated considering a genomic mutation rate of 2.8×10^{-9} per site per generation and a one-year generation time. Branch colours correspond to the predominant genetic cluster to which each population was assigned based on STRUCTURE analyses for $K = 6$ (see Figure 3b) and background colours indicate geological divisions of the Quaternary. The taxonomic status of populations before (input; ? = unknown) and after (output) species delimitation analyses in DELINEATE is shown on the right; DELINEATE uses the ultrametric phylogeny inferred with BPP together with prior species assignments for a subset of populations (input) to evaluate whether the remaining populations belong to previously described species or represent distinct lineages. Population codes as described in Table 1. The inset image shows a male of the short-winged *C. pulloides* (illustration by Marina Trillo).

pronotum-head of male specimens, two taxonomically relevant traits in the genus *Chorthippus* (Noguerales et al., 2018; Willemse et al., 2009). This approach is particularly relevant given that a previous morphology-based study reported that some populations of the complex in the Peloponnese Peninsula exhibit intermediate phenotypes, potentially reflecting morphological transitions, incipient speciation, or ongoing or historical hybridization among taxa in the region (Willemse et al., 2009). For geometric and linear morphometric analyses, we captured images of the forewing, pronotum-head and hind femur of each male specimen using a Leica Flexacam C3 camera mounted on a Zeiss Stemi 2000 stereomicroscope.

Shape variation analyses

We digitized homologous landmarks from each photograph using the R v. 4.2.3 (R Core Team, 2021) package 'StereoMorph' (Olsen & Westneat, 2015). We identified 12 landmarks for the forewing (Figure 1a, Table S1) and 20 landmarks for the pronotum-head combined (Figure 1b, Table S1). We used Generalized Procrustes Analyses (GPA; Rohlf, 1998) implemented in the R package 'geomorph' (Adams & Otárola-Castillo, 2013) to remove the effects of scale, rotation and translation of all landmark configurations. To evaluate shape variation both with and without the influence of body size, we conducted analyses on both raw and size-adjusted Procrustes coordinates. Size correction was achieved by fitting a Procrustes linear model (*ProcD.lm*) with shape as the response variable and centroid size as the predictor. The residuals of this model, representing shape variation independent of size, were used for size-corrected analyses. Then, we performed principal component analyses (PCA) on the covariance matrix of Procrustes-aligned data to identify the major axes of shape variation among individuals and summarize patterns of morphological variation for the two traits. We used the function *ProcD.lm* in the R package 'geomorph' to perform a Procrustes ANOVA

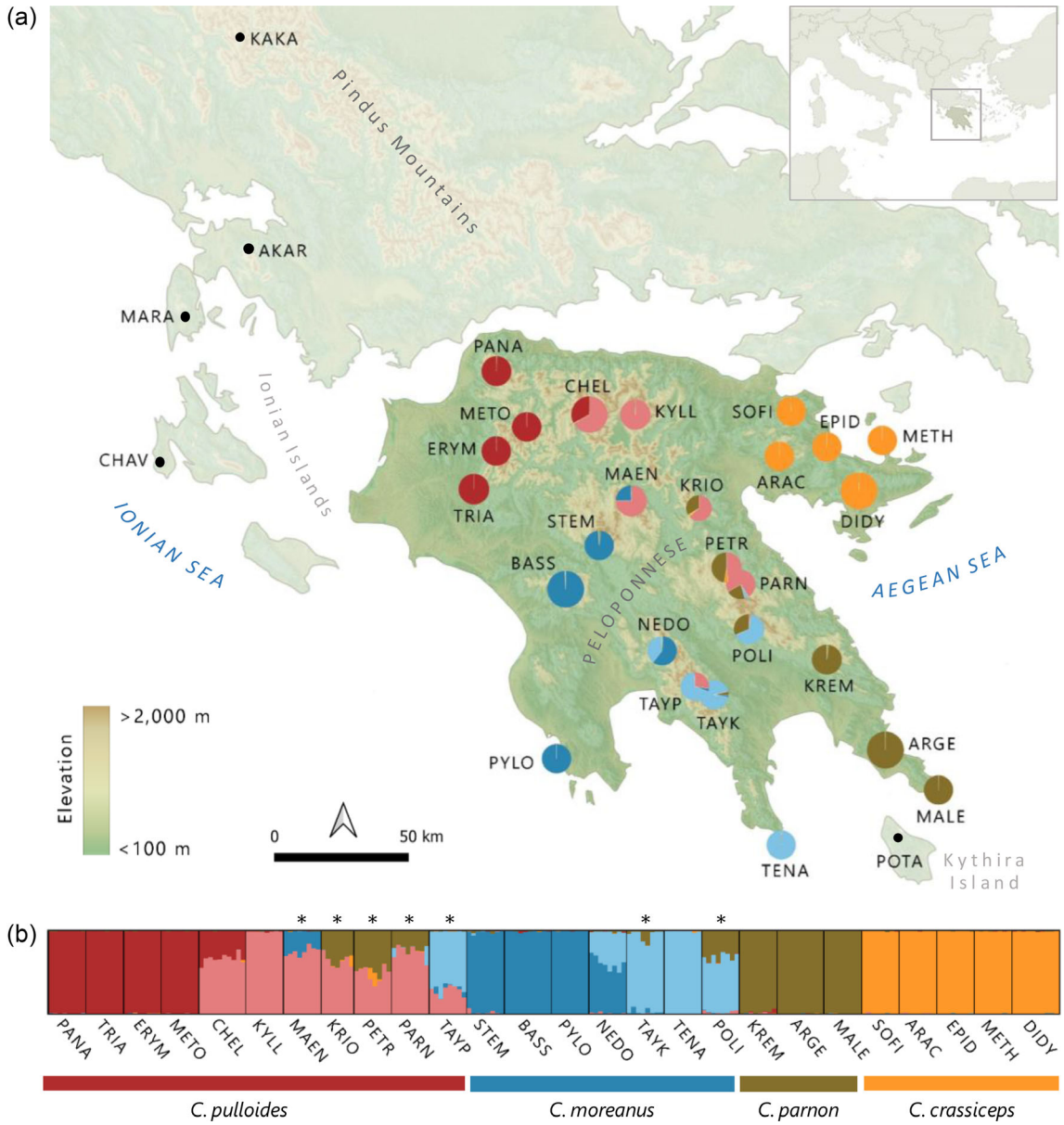

FIGURE 3 (a) Geographic distribution of the studied populations of the *Chorthippus* species complex in Greece and (a, b) results of genetic assignments based on STRUCTURE for the populations distributed within the Peloponnese Peninsula. (a) Pie charts on map show the geographic location of genotyped populations within the Peloponnese Peninsula and their respective genetic assignments for $K = 6$. (b) In barplots, each individual is represented by a vertical bar partitioned into K coloured segments showing the individual's probability of belonging to the cluster with that colour; thin vertical black lines separate individuals from different populations. Populations marked with an asterisk correspond to admixed populations identified by STRUCTURE and excluded from phylogenomic analyses (see Species delimitation analyses). Population codes as described in Table 1.

(Anderson, 2001) and assess differences in shape among taxa and populations (Adams & Otárola-Castillo, 2013). Finally, we used the function *pairwise* in the R package 'rrpp' to calculate the distance and corresponding empirically derived *p*-values among taxa and populations using a nonparametric randomized residual permutation procedure (Collyer & Adams, 2018). Due to limited sampling in two localities (KRIO: $n = 2$; STEM: $n = 1$; Table 1), these populations were excluded from population-level comparisons but retained in the PCA to visualize their affinities with other populations.

Relative wing size analyses

We assessed wing size variation by calculating the ratio between forewing length and femur length (FWL/FL). This trait has been widely used in taxonomic and ecological studies as a proxy for relative wing development and potential dispersal capacity (Noguerales et al., 2018; Noguerales & Ortego, 2022). Linear distances were extracted from digitized landmark coordinates using the *interlmkdist* function from the R package 'geomorph' (Anderson, 2001). Forewing length

was measured between landmarks 1 and 12 (Figure 1a, Table S1). We used femur length as a proxy for overall body size, as it correlates strongly with structural body length in grasshoppers (García-Navas et al., 2017b; Ortego et al., 2012). The resulting FWL/FL ratios were compared among populations using ANOVA and post hoc Tukey's tests. To visualize the distribution and overlap of FWL/FL ratios across taxa and populations, we generated density ridge plots using the R package 'ggplot2'.

RESULTS

Genomic datasets

After the different quality filtering steps, the average number of reads retained per individual was 3,128,441 (range = 858,283–6,270,222). Attributes of the different genomic datasets used for all downstream analyses are presented in Table S2. All datasets have been deposited in Figshare (https://doi.org/10.6084/m9.figshare.31136593; Ortego & Trillo, 2026).

Phylogenomic inference and divergence time estimation

Phylogenetic reconstructions obtained with BPP and RAXML yielded similar topological relationships, with minor differences involving recently diverged populations of *C. parnon* (Figures 2 and S1). Phylogenetic analyses revealed that the population of *C. pulloides* from Mount Kakarditsa (KAKA) constitutes a highly divergent lineage, which is sister to a clade comprising all other taxa and populations within the complex. This latter clade splits into two major subclades: one includes the population of *C. pulloides* from Mount Akarnanika (AKAR) and two sister lineages of the Ionian island-endemic *C. sangiorgii* (MARA and CHAV), hereafter referred to as the Central Greece-Ionian Islands clade; the other encompasses all populations and taxa from the Peloponnese Peninsula, as well as the population of *C. parnon* from the adjacent Kythira Island (POTA), hereafter referred to as the Peloponnese-Kythira Island clade. Within the Peloponnese-Kythira Island clade, all populations of *C. pulloides* from northern Peloponnese formed a monophyletic group, which was sister to a clade including the remaining populations and taxa in this group. This latter clade comprised *C. moreanus*, which was sister to a clade containing *C. parnon* and *C. crassiceps*. All populations of *C. moreanus* and *C. crassiceps* formed reciprocally monophyletic clades. However, the population of *C. parnon* from Kythira Island (POTA) was sister to a clade including both *C. crassiceps* and the remaining populations of *C. parnon*, rendering *C. parnon* paraphyletic (Figures 2 and S1). Overall, node support was high across the tree inferred by BPP (Bayesian posterior probabilities >0.99), with lower values restricted to some shallow divergences among populations within *C. moreanus*, *C. parnon* and *C. crassiceps* (Figure 2). Node support in the tree inferred by RAXML was high (bootstrap support >94%) for most nodes, except those separating the Central Greece–Ionian Islands and Peloponnese–Kythira Island clades and *C. sangiorgii* from the lineage of *C. pulloides* from Mount Akarnanika (AKAR) (Figure S2). In the RAXML tree including all populations (i.e., without excluding admixed populations), the putative hybrid populations occupy basal positions within their respective clades, as expected when admixed populations are included in phylogenetic analyses (Figure S3).

Molecular dating analyses indicate that all lineages and putative taxa diverged during the Middle Pleistocene (Chibanian Stage, 0.71–0.18 Ma BP; Figure 2). The earliest divergence corresponds to the split between the lineage of *C. pulloides* from Mount Kakarditsa (KAKA) and the rest of the taxa and populations (ca. 0.71 Ma BP), followed by the divergence between the Central Greece–Ionian Islands and Peloponnese–Kythira Island clades (0.35 Ma BP; Figure 2). The Ionian Island-endemic *C. sangiorgii* diverged from the *C. pulloides* lineage from Mount Akarnanika (AKAR) around 0.3 Ma BP, whereas all lineages and putative taxa within the Peloponnese–Kythira Island clade diverged more recently, between approximately 0.28 and 0.18 Ma BP (Figure 2).

Species delimitation analyses

Species delimitation analyses in DELINEATE identified three previously unrecognized species. Two populations originally assigned to *C. pulloides* (KAKA and AKAR) and the population from Kythira Island (POTA), initially assigned to *C. parnon*, were inferred to represent distinct evolutionary lineages consistent with separate species (*DelineatedSp001*, *DelineatedSp002* and *DelineatedSp003*) (Figures 2 and S1, Table 1). All remaining populations were assigned to their nominal species, including those of *C. crassiceps*, which formed a well-supported monophyletic group. Species delimitation inferences were consistent across the slightly different topologies obtained with BPP (Figure 2) and RAXML (Figure S2).

Testing for introgression

D-statistic tests revealed significant genetic introgression (i) from *C. moreanus* into *C. pulloides* populations of Mt. Maenalon (MAEN) and Mt. Taygetus (TAYP); (ii) from *C. parnon* into several *C. pulloides* populations located near their distributional boundaries (KRIO, PETR and PARN); and (iii) from *C. parnon* into the *C. moreanus* population from Polidroso (POLI) (Table S3). Although STRUCTURE analyses indicated that the *C. moreanus* population from Mt. Taygetus (TAYK) exhibits signatures of genetic admixture with *C. parnon* (see Population genetic structure), the *D*-statistic test did not detect significant genetic introgression for this population (Table S3).

Population genetic structure

STRUCTURE analyses including all populations and taxa showed that ΔK peaked at $K = 2$ and exhibited a secondary peak at $K = 6$, whereas

LnPr(X|*K*) reached a plateau at $K = 6–7$ (Figure S4). Genetic clusters inferred for $K = 2–5$ were inconsistent with phylogenomic analyses and current taxonomic assignment of populations (see Figure S5), likely reflecting uneven population sampling across taxa and lineages (Puechmaille, 2016) and/or the limited ability of STRUCTURE to recover higher-level relationships when individuals from large datasets with complex evolutionary histories are forced into too few clusters (Funk et al., 2020; Kalinowski, 2011; e.g., Ortego et al., 2025).

From $K = 5$ to $K = 7$, STRUCTURE analyses showed a hierarchical splitting of taxa and lineages within taxa that was broadly congruent with phylogenomic inferences (Figures 2 and 3). At $K = 6$, STRUCTURE identified two genetic clusters within *C. pulloides* (dark red and light red), two clusters within *C. moreanus* (dark blue and light blue), and single clusters corresponding to *C. parnon* (brown) and *C. crassiceps* (orange). Several groups emerged as genetically homogeneous and cohesive, notably *C. crassiceps* (SOFI, EPID, ARAC, METH and DIDY) and the southeastern populations of *C. parnon* (KREM, ARGE and MALE).

In contrast, many populations from the central and southern Peloponnese showed clear signals of admixture among genetic clusters, consistent with their geographic location near the boundaries of taxa distributions (i.e., historical contact zones; Figure 3a). The most noticeable cases involved *C. pulloides* populations from the central and southern Peloponnese, which exhibited varying degrees of admixture with *C. moreanus* (MAEN and TAYP) and *C. parnon* (KRIO, PETR and PARN). Approximately 25% of the inferred ancestry of the putative *C. pulloides* population from Mt. Maenalon (MAEN) originated from the western lineage of *C. moreanus*. Likewise, ca. 70% of the inferred ancestry of the putative *C. pulloides* population from Mt. Taygetus (TAYP) was estimated to derive from the eastern lineage of *C. moreanus*. Between 20% and 50% of the ancestry of *C. pulloides* populations from Mt. Parnon and surrounding areas (KRIO, PETR and PARN) originated from *C. parnon*. Finally, *C. moreanus* populations located at the foothills of Mt. Taygetos (TAYK) and Mt. Parnon (POLI) presented ca. 5% and 32% of genetic introgression from *C. parnon*, respectively.

Timing of divergence and admixture

The model best explaining the formation of hybrid populations was a scenario of divergence in strict isolation followed by an admixture event (Model A; Figure S1), with the alternative model receiving comparatively lower support (ΔAIC > 1.8; Table 2). Divergence between *C. pulloides* and *C. moreanus* (KYLL–MAEN–PYLO, point estimate: 452 ka; 95% CI: 454–498 ka; KYLL–TAYP–TENA, point estimate: 427 ka; 95% CI: 428–473 ka) and between *C. pulloides* and *C. parnon* (KYLL–PARN–MALE, point estimate: 374 ka; 95% CI: 381–424 ka) was inferred to have occurred during the Middle Pleistocene (Table 3). The admixture events that led to the formation of hybrid populations took place considerably later, ranging from ca. 84 ka for PARN (95% CI: 83–91 ka) to ca. 103 ka for MAEN (95% CI: 100–107 ka), except in TAYP where admixture was notably older, dating back to ca. 253 ka (95% CI: 232–249 ka) (Table 3). Across triplets, the proportion of ancestry in admixed populations derived from *C. pulloides* was consistently higher than that from the other parental species, ranging from 69.1% in PARN (95% CI: 67.8–69.2%) to 84.3% in TAYP (95% CI: 82.6–84.2%), with MAEN showing an intermediate value of 78.0% (95% CI: 77.5–78.6%) (Table 3).

Morphometric analyses

Geometric morphometric analyses of forewing shape based on raw Procrustes coordinates showed a clear separation between short- and long-winged taxa, with populations of *C. pulloides* and *C. sangiorgii* clustering apart from *C. moreanus* and *C. parnon* (Figure S6a). Populations of *C. crassiceps* exhibited substantial variation in wing size, with northwestern populations (SOFI, ARAC) showing shorter wings and grouping with *C. pulloides* and *C. sangiorgii*, and southeastern populations (METH, DIDY) displaying longer wings and clustering with *C. moreanus* and *C. parnon* (Figure S6a). The EPID population occupied an intermediate position in morphospace, consistent with a continuous geographical cline in wing development (Figure S6a). Populations of *C. pulloides* presenting genetic admixture with *C. moreanus* (MAEN, TAYP) or *C. parnon* (PARN) exhibited forewing shapes indistinguishable from those of non-admixed populations of *C. pulloides* (Figure S6a). Allometric analyses indicated that size had a significant effect on forewing shape (one-way ANOVA; $F_{1,111} = 304.49$, $p < 0.001$). After correcting for size effects, shape differences between short- and long-winged taxa were no longer apparent (Figure S6b). For pronotum–head shape, size also had a significant effect (one-way ANOVA; $F_{1,111} = 5.47$, $p = 0.002$), and overall variation among taxa was limited, with most populations broadly overlapping in morphospace (Figure S7a,b). Procrustes distances for both traits were generally small and non-significant in most pairwise comparisons (Tables S4 and S5), indicating weak shape differentiation among populations. At the species level, forewing shape also showed low Procrustes distances overall (Table S6), with significant values detected in only a limited number of comparisons, mostly involving the most divergent lineages (AKAR and KAKA). For pronotum–head shape, significant differences were likewise limited and mainly restricted to contrasts involving *C. sangiorgii* and AKAR (Table S7).

Relative forewing size (FWL/FL) varied markedly among taxa, with two main morphotypes identified: short-winged *C. sangiorgii* and *C. pulloides*, and long-winged *C. moreanus* and *C. parnon* (Figure 4). As noted above, *C. crassiceps* exhibited substantial population-level variation in relative wing size, following a northwest–southeast cline from short-winged (SOFI and ARAC) to long-winged (METH and DIDY) populations, with intermediate values in a geographically transitional population (EPID) (Figure 4). Post hoc pairwise comparisons revealed significant differences in FWL/FL ratios for most population pairs, particularly between short- and long-winged groups (Table S8), and species-level comparisons showed a similar pattern (Table S9). Notably, admixed populations putatively assigned to *C. pulloides* (MAEN, PETR, PARN and TAYP) exhibited FWL/FL values overlapping those of genetically pure populations of this taxon (Figures 3 and 4).

DISCUSSION

Our integrative analyses on the *Chorthippus* species complex from Greece provide new insights into the processes shaping lineage diversification and the persistence of species boundaries in the Mediterranean biodiversity hotspot. Phylogenomic reconstructions indicate that diversification occurred during the Middle Pleistocene, with subsequent events of secondary contact generating complex patterns of genetic structure and admixture across the Peloponnese. Genetic clustering analyses are broadly consistent with the geographic ranges of the four taxa in the region, but species boundaries become diffuse at distributional margins, where several populations exhibit clear signatures of historical hybridization, revealing semi-permeable species boundaries. Together, these findings emphasize the interplay between historical isolation, secondary contact and incomplete reproductive isolation as key drivers of diversification within this complex, underscoring the Mediterranean region as a major centre of microgeographic speciation and a remarkable reservoir of endemism.

Species delimitation under recent divergence and incomplete lineage sorting

Phylogenomic analyses revealed a highly divergent lineage corresponding to the putative northernmost population of *C. pulloides* from Mt. Karkarditsa (KAKA), which was recovered as sister to a clade including all other taxa (Figures 2 and S1). Within this latter clade, two geographically coherent subclades were identified: a Central Greece-Ionian Islands clade, comprising *C. sangiorgii* and the putative population of *C. pulloides* from the Acarnanian Mountains (AKAR), and a Peloponnese-Kythira Island clade including *C. moreanus*, *C. parnon*, *C. crassiceps*, and the remaining populations of *C. pulloides* (Figures 2 and S1). This deep split separates populations distributed north and south of the Corinthian Gulf, a well-known biogeographic barrier that has shaped divergence in multiple Balkan organisms (Collier & Dart, 1991; Kiourtsoglou et al., 2021; Ortego et al., 2026). The isolation of the Peloponnese Peninsula from the rest of mainland Greece since the Pliocene likely promoted the differentiation of the Peloponnese-Kythira clade, whereas lineages north of the Corinthian Gulf diversified within Central Greece and the Ionian Islands. Consistent with this scenario, paleodistribution modelling for the partially co-distributed alpine grasshopper genus *Oropodisma* indicates that the Peloponnese Peninsula has remained disconnected from the rest of the Balkans at least since the Last Glacial Maximum, supporting its isolation during the late Pleistocene (Ortego et al., 2026). Beyond this primary north–south division, the complex internal topography of the Peloponnese appears to have further contributed to diversification within this region. The southern sub-peninsulas—Messenian, Mani, Cape Malea and Argolid—constitute geographic cul-de-sacs where genetically most pure populations of *C. moreanus*, *C. parnon* and *C. crassiceps* are found. These narrow peninsulas likely acted as isolation pockets, or 'refugia within refugia', during the Pleistocene, as reported for other taxa (Allegrucci et al., 2021; Kiourtsoglou et al., 2021; Nieto-Feliner, 2011; Thanou et al., 2023), underscoring their role in promoting local divergence and speciation. The concordance of our results with previously documented phylogeographic patterns supports a predominantly geographic dimension of diversification in the complex. Within the Peloponnese Peninsula, populations assigned to each putative taxon were reciprocally monophyletic with strong node support, indicating that our dataset provided sufficient phylogenetic signal to resolve evolutionary relationships despite the recent divergence of lineages. Only a few nodes separating conspecific populations showed low support, likely reflecting incomplete lineage sorting (ILS) resulting from recent divergence.

Divergence time estimates place the deepest nodes within the Middle Pleistocene (<0.7 Ma), consistent with estimates for other complexes of Mediterranean grasshoppers, in which genuine speciation events involving genotypically cohesive taxa with evidence of total (Ortego et al., 2021, 2024) or partial reproductive isolation (Ortego & Knowles, 2022; Ortego et al., 2026) occurred within the last 0.3–1.5 Ma. Accordingly, the genetic divergence and phenotypic differentiation inferred within the *Chorthippus* complex in Greece are best interpreted as the outcome of recent or incipient speciation processes rather than as mere genetic discontinuities resulting from geographical barriers to dispersal. Our results also help resolve taxonomic uncertainties within the group. Early assessments noted the strong morphological similarity between *C. sangiorgii* and *C. pulloides*, leading some authors to suggest that both taxa might represent a single species (Ramme, 1926, 1927; Willemse, 1984, 1985, 1986). Subsequent bioacoustic studies revealed a distinctive song in *C. pulloides*, providing evidence for its differentiation from *C. sangiorgii* (Willemse et al., 2009). Our phylogenomic analyses further corroborate that both taxa represent evolutionary independent lineages (Figure 2), illustrating how recent divergence and limited phenotypic differentiation can generate taxonomic uncertainty in this group. Species delimitation analyses in DELINEATE largely matched current taxonomy but also revealed three additional distinct lineages (KAKA, AKAR and POTA) (Figure 2), corresponding to populations that in some cases (AKAR) had previously been regarded as morphologically transitional forms (Willemse et al., 2009). Despite their close morphological resemblance to *C. pulloides* (KAKA, AKAR) or *C. parnon* (POTA), these populations were consistently recovered as independent evolutionary entities. Together, these findings illustrate how morphologically uniform taxa may conceal substantial hidden diversity, a pattern frequently documented in recent Pleistocene radiations (i.e., cryptic species; Bickford et al., 2007; e.g., Huang et al., 2020; Ortego et al., 2024).

Hybridization dynamics in secondary contact zones

D-statistic tests and STRUCTURE analyses revealed that historical hybridization and genetic admixture within the complex are geographically restricted and largely confined to populations located at the margins of species ranges (Figure 3; Table S3). Most admixture events involved short-winged *C. pulloides* from the central and southern Peloponnese, whose populations occur within or adjacent to the distributional ranges of the long-winged *C. moreanus* and *C. parnon*. These analyses

TABLE 2 Alternative models of divergence and admixture tested using FASTSIMCOAL2 for three population triplets including hybrid populations (MAEN, PARN, TAYP) and representative populations of their parental taxa *C. pulloides* (KYLL) and *C. moreanus* (PYLO, TENA) or *C. parnon* (MALE).

		KYLL-MAEN-PYLO (704 SNPs)				KYLL-PARN-MALE (625 SNPs)				KYLL-TAYP-TENA (466 SNPs)			
Model	***k***	**lnL**	**AIC**	**ΔAIC**	**ω_i**	**lnL**	**AIC**	**ΔAIC**	**ω_i**	**lnL**	**AIC**	**ΔAIC**	**ω_i**
Model A	**8**	**-1129.71**	**2275.41**	**0.00**	**0.00**	**-1015.09**	**2046.18**	**0.00**	**0.00**	**−720.31**	**1456.61**	**0.00**	**0.00**
Model B	12	−1126.80	2277.61	2.19	0.00	−1012.00	2047.99	1.81	0.00	−717.45	1458.90	2.28	0.00

Note: Models include scenarios of divergence in strict isolation followed by an admixture event (Model A), and divergence in strict isolation followed by an admixture event and contemporary gene flow (Model B) (see Figure S1). Population codes as described in Table 1. The best-supported scenario is highlighted in bold. The number of variable single-nucleotide polymorphisms (SNPs) retained to calculate the site frequency spectrum is indicated in parentheses.

Abbreviations: ΔAIC, difference in AIC value from that of the strongest model; AIC, Akaike's information criterion value; *k*, number of parameters in the model; lnL, maximum likelihood value of the model; ω_i, AIC weight.

TABLE 3 Parameters inferred from coalescent simulations with FASTSIMCOAL2 under the most supported scenarios of divergence and admixture tested using FASTSIMCOAL2 for three population triplets including hybrid populations (MAEN, PARN, TAYP) and representative populations of their parental taxa *C. pulloides* (KYLL) and *C. moreanus* (PYLO, TENA) or *C. parnon* (MALE).

KYLL-MAEN-PYLO				KYLL-PARN-MALE				KYLL-TAYP-TENA			
Parameter	**Point estimate**	**Lower bound**	**Upper bound**	**Parameter**	**Point estimate**	**Lower bound**	**Upper bound**	**Parameter**	**Point estimate**	**Lower bound**	**Upper bound**
θ_{ANC}	284,977	244,302	270,144	θ_{ANC}	252,274	222,751	249,655	θ_{ANC}	569,690	448,498	490,887
$\theta_{ANC\text{-}KYLL}$	350,405 250,332 299,724	339,536	376,468	$\theta_{ANC\text{-}KYLL}$	289,927	285,379	322,417	$\theta_{ANC\text{-}KYLL}$	242,404	250,332	299,724
$\theta_{ANC\text{-}PYLO}$	236,831	229,958	256,249	$\theta_{ANC\text{-}MALE}$	198,824	196,826	225,076	$\theta_{ANC\text{-}TENA}$	135,552	145,112	177,692
θ_{KYLL}	759,677	–	–	θ_{KYLL}	759,677	–	–	θ_{KYLL}	759,677	–	–
θ_{MAEN}	574,315	551,021	598,160	θ_{PARN}	415,440	408,995	455,342	θ_{TAYG}	762,130	675,924	743,458
θ_{PYLO}	290,163	278,144	307,204	θ_{MALE}	374,729	377,270	417,702	θ_{TENA}	591,031	541,960	603,004
r	0.780	0.775	0.786	*r*	0.691	0.678	0.692	*r*	0.843	0.826	0.842
T_{DIV}	452,165	454,768	498,160	T_{DIV}	373,742	380,909	424,008	T_{DIV}	427,251	427,893	472,906
T_{ADMIX}	102,550	100,052	106,627	T_{ADMIX}	84,100	82,580	90,792	T_{ADMIX}	252,517	232,377	249,480

Note: Population codes as described in Table 1. The table shows point estimates and lower and upper 95% confidence intervals for each parameter, including mutation-scaled ancestral and contemporary effective population sizes (θ), the proportion of lineages inherited from *C. pulloides* (*r*) and the timing of divergence (T_{DIV}) and admixture (T_{ADMIX}), assuming one generation per year. Contemporary effective population size of *C. pulloides* (θ_{KYLL}) was calculated from its levels of nucleotide diversity (π) and fixed in FASTSIMCOAL2 analyses to enable the estimation of all other parameters (see Testing for introgression for further details). Models are illustrated in Figure S1.

also uncovered strongly asymmetric introgression, with gene flow occurring predominantly from long-winged *C. moreanus* and *C. parnon* into the brachypterous *C. pulloides*. This pattern is consistent with differences in dispersal ability, whereby the long-winged taxa are more likely to reach the range and hybridize with *C. pulloides*, whereas movements in the opposite direction are likely constrained, mirroring patterns reported in other hybridizing grasshoppers with contrasting dispersal capacities (Ortego et al., 2021; Ortego & Knowles, 2022). In addition, the broader geographic distributions of *C. moreanus* and *C. parnon* may promote genetic swamping of the geographically more restricted populations of *C. pulloides*. This dynamic is exemplified on Mt. Taygetus, where populations of *C. pulloides* show high levels of admixed ancestry with *C. moreanus*, while no evidence of reciprocal introgression is detected, despite both taxa occurring less than 1.7 km apart.

The altitudinal distribution of *C. pulloides* across its range provides further insight into the mechanisms enabling lineage persistence despite weak reproductive barriers. In the northern Peloponnese, where other members of the complex are absent and opportunities for hybridization are minimal, *C. pulloides* occupies a broad elevational range (400–2400 m). In contrast, in the central and southern Peloponnese *C. pulloides* is largely restricted to high elevations (>1800 m), whereas *C. moreanus* and *C. parnon* dominate surrounding foothills and lowlands. This altitudinal segregation likely underpins the persistence of highly isolated *C. pulloides* populations on Mt. Maenalon, Mt. Parnon and Mt. Taygetus by limiting lineage fusion and genetic swamping by the more widespread lowland taxa. The relatively high levels of admixed ancestry detected in these *C. pulloides* populations suggest that repeated downslope shifts during glacial periods facilitated secondary contact and hybridization with long-winged taxa at

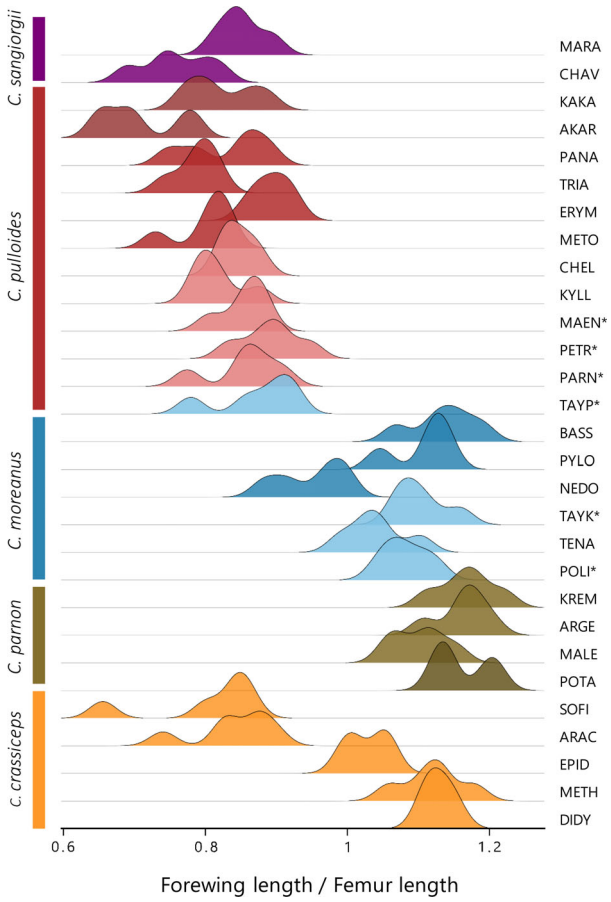

FIGURE 4 Distribution of forewing-to-femur length ratios (FWL/FL) of males across the studied populations of the *Chorthippus* species complex in Greece. Ridge density plots represent variation in relative wing size, with femur length used as a proxy for body size. Populations are coloured according to their corresponding lineages in the phylogenetic tree (Figure 1) or the main genetic cluster to which genetically admixed populations (marked with an asterisk) were assigned based on STRUCTURE analyses (Figure 3). Population codes as described in Table 1.

local to regional scales within the Peloponnese, whereas subsequent interglacials drove admixed populations back to alpine and subalpine habitats. Consistent with this scenario, coalescent estimates from FASTSIMCOAL2 date admixture pulses to the Late Pleistocene (ca. 250–80 ka; Table 3), coinciding with major glacial–interglacial cycles (Hewitt, 1996, 2000; Hughes et al., 2006). Notably, the admixture event inferred for TAYP appears substantially older (ca. 253 ka) than those estimated for PETR and PARN (ca. 84–103 ka; Table 3), indicating that major episodes of secondary contact and hybridization occurred asynchronously across populations. This scenario is further supported by paleoclimate-based reconstructions of historical distributions in other co-distributed alpine grasshoppers, which experienced range expansions during glacial periods and contractions to mountain tops during warm interglacials (Ortego et al., 2026). These shifts were largely elevational, which may explain why genetic admixture is spatially restricted and exclusively observed among geographically adjacent lineages (Figure 3). Altogether, these results illustrate how Quaternary climatic oscillations promoted repeated secondary contacts among lineages that are currently distributed in allopatry, generating localized hybrid zones (Hewitt, 1996, 2000; Ortego & Knowles, 2022).

Morphological variation along the speciation continuum

Our morphometric analyses show that forewing and pronotum-head shapes are largely conserved across lineages (Figures S5 and S6, Tables S4 and S5), with wing length relative to body size being the only trait that shows partial concordance with taxonomic boundaries (Figure 4, Table S9). This overall morphological conservatism is consistent with expectations under cryptic speciation (Bickford et al., 2007) and suggests pronounced morphological stasis, except in traits directly associated with dispersal. Comparable patterns have been reported in other Orthoptera, where syntopic and reproductively isolated lineages remain morphologically indistinguishable (Ortego et al., 2024) or differ primarily in dispersal-related traits (Ortego et al., 2021).

The evolutionary history of Pterygota is marked by repeated transitions in wing development (e.g., from macroptery to brachyptery or aptery), often associated with habitat stability and reduced dispersal requirements (Roff, 1990, 1994; Zera & Denno, 1997). Assuming a long-winged ancestral state, our phylogeny reveals at least four independent reductions in wing size within the complex (Figure 2): (i) in the isolated KAKA lineage, (ii) in the ancestor of *C. sangiorgii* and the mainland AKAR lineage; (iii) in *C. pulloides*; and (iv) more recently within *C. crassiceps*, which includes both short-winged and long-winged subclades. These repeated reductions highlight the evolutionary lability of dispersal-related traits, consistent with patterns documented in other Orthoptera (Ortego et al., 2021). The taxon *C. crassiceps* provides a particularly clear example of an ongoing evolutionary transition in dispersal ability. Within this species, wing length displays a pronounced northwest-southeast cline: short-winged populations (SOFI, ARAC) occur in the northwest part of its range, long-winged populations (METH, DIDY) in the southeast, and intermediate forms (EPID) in the intervening area (Figure 4). Northwestern and southeastern populations form distinct subclades in our phylogenomic analyses (Figure 2), indicating that variation in wing length reflects an evolutionary shift in flight capacity rather than phenotypic plasticity or simple polymorphism. Divergence-time estimates indicate that these subclades separated <120 ka and are distributed across <35 km, illustrating how substantial changes in dispersal-related morphology can evolve over short spatial and temporal scales. Similar rapid losses of flight ability have been documented in other grasshoppers (Ortego et al., 2021) and in other insect groups (McCulloch et al., 2022; Suzuki et al., 2019). Collectively, these results demonstrate how transitions toward brachyptery can evolve rapidly in fragmented landscapes, even across relatively small geographic distances.

Analysis of admixed populations resulting from hybridization between short-winged (*C. pulloides*) and long-winged (*C. moreanus* or *C. parnon*) taxa provides further insight into the drivers of wing-size

reduction in the complex. Despite substantial genomic admixture with long-winged taxa (Figure 3), all hybrid populations retain the brachypterous phenotype characteristic of genetically pure *C. pulloides* (Figure 4). The absence of phenotypically intermediate populations, together with the persistence of a *C. pulloides*-like morphology despite extensive introgression, suggests strong selection against long-winged phenotypes in the high elevation habitats predominantly occupied by *C. pulloides* in the central and southern Peloponnese and/or phenotypic assimilation through repeated backcrossing with the taxon contributing most to the hybrid genome (Huang, 2016; Ortego et al., 2026; Rheindt et al., 2014).

CONCLUSIONS

Our study illustrates how the integration of genomic and morphometric data can clarify taxonomic boundaries in recently diversified species complexes. In the *Chorthippus* species complex from Greece, genomic evidence reveals a mosaic of differentiation and admixture operating across multiple temporal and spatial scales: most taxa exhibit well-defined genetic structure, whereas extensive hybridization occurs at their distributional margins. Divergence within the complex was likely promoted by spatial isolation associated with the complex topography and range shifts driven by Pleistocene climatic oscillations (Carstens & Knowles, 2007; Hewitt, 2000), and subsequently reshaped by episodes of secondary contact and introgressive hybridization (Ortego & Knowles, 2022; Seehausen, 2004; Figures 3 and S2). Within this dynamic context, the southern Peloponnesian sub-peninsulas—harbouring the genetically purest populations of several taxa—illustrate how small-scale topographic cul-de-sacs can act as long-term microrefugia, maintaining lineage independence through repeated climatic fluctuations. Recurrent and independent reductions in wing length, contrasted with the strong conservation of other morphological traits (e.g., pronotum-head and forewing shape), identify dispersal-related morphology as a primary axis of divergence under otherwise pronounced morphological stasis (Roff, 1990, 1994; Zera & Denno, 1997). This combination of partial reproductive isolation and morphological conservatism highlights the challenges of species delimitation in topographically heterogeneous Mediterranean landscapes (García-Navas et al., 2017a; Hawlitschek et al., 2022; Neumeister et al., 2025; Noguerales et al., 2018; Ortego et al., 2024; Schmidt et al., 2024).

Our results further show that recent divergence coupled with morphological uniformity can mask substantial hidden diversity. Accordingly, several geographically restricted lineages (e.g., AKAR, KAKA and POTA) display clear genomic distinctiveness despite minimal morphological differentiation, illustrating how geographic isolation and reduced dispersal capacity can promote fine-scale cryptic diversification. From a conservation perspective, our findings are particularly relevant, as they identify multiple cryptic evolutionary units and refine the taxonomic status and distributions of several taxa within the complex (*C. pulloides*, *C. parnon*, *C. crassiceps*) currently listed as 'Near Threatened' on the IUCN Red List (Tzortzakaki et al., 2023a, 2023b, 2023c). Notably, while these lineages are well-differentiated at the genomic level, we have chosen not to make formal taxonomic decisions at this stage, given the unresolved status of the genus *Chorthippus* and the need for additional evidence from broader phylogenomic and phenotypic analyses. Future work integrating additional genomic data and complementary phenotypic traits (e.g., internal genitalia) will be critical to clarify the taxonomic status of these lineages, and may allow their recognition as distinct taxa once further lines of evidence are available. In the meantime, our results provide a robust framework to prioritize these lineages for conservation and further evolutionary study. Overall, our study advances understanding of how semi-permeable species boundaries, dispersal-related traits and topographic complexity interact to shape diversification in the Mediterranean biodiversity hotspot.

AUTHOR CONTRIBUTIONS

Marina Trillo: Conceptualization; data curation; formal analysis; investigation; methodology; validation; visualization; writing—original draft. **Joaquín Ortego:** Conceptualization; data curation; funding acquisition; investigation; methodology; project administration; resources; supervision; validation; visualization; writing—review and editing.

ACKNOWLEDGEMENTS

We thank Ioannis Anastasiou (National and Kapodistrian University of Athens, Greece) for supporting our research permit applications and Anna Papadopoulou and Jorge Gutiérrez-Rodríguez for their help during fieldwork. We also thank three anonymous referees for their constructive and valuable comments on an earlier version of the manuscript. Sampling permits were granted by the Ministry of the Environment and Energy from Greece (permit nos. YPEN/DDD/34736/1134 and YPEN/DDD/32363/1054). Logistic support was provided by Laboratorio de Ecología Molecular (LEM-EBD) from Estación Biológica de Doñana (CSIC). We also thank Centro de Supercomputación de Galicia (CESGA) and Doñana's Singular Scientific-Technical Infrastructure (ICTS-RBD) for access to computer resources.

FUNDING INFORMATION

Grant TED2021-129328B-I00 funded by Ministerio de Ciencia e Innovación (MCIN/AEI/10.13039/501100011033) and European Union NextGenerationEU/PRTR; Grant PID2021-123298NB-I00 funded by Ministerio de Ciencia e Innovación and European Regional Development Fund (MCIN/AEI/10.13039/501100011033/FEDER, UE).

CONFLICT OF INTEREST STATEMENT

The authors declare no conflicts of interest.

DATA AVAILABILITY STATEMENT

Raw Illumina reads have been deposited at the NCBI Sequence Read Archive (SRA) (https://www.ncbi.nlm.nih.gov/) under BioProject PRJNA702631. Input files for all analyses are available in Figshare at https://doi.org/10.6084/m9.figshare.31136593 (Ortego & Trillo, 2026).

ETHICS STATEMENT

All samples were obtained under permits granted by the Greek Ministry of the Environment and Energy (permit nos. YPEN/DDD/34736/1134 and YPEN/DDD/32363/1054).

ORCID

Marina Trillo https://orcid.org/0000-0002-3650-138X
Joaquín Ortego https://orcid.org/0000-0003-2709-429X

REFERENCES

Adams, D.C. & Otárola-Castillo, E. (2013) Geomorph: an R package for the collection and analysis of geometric morphometric shape data. *Methods in Ecology and Evolution*, 4(4), 393–399. Available from: https://doi.org/10.1111/2041-210X.12035

Allegrucci, G., Rampini, M., Chimenti, C., Alexiou, S. & Di Russo, C. (2021) *Dolichopoda* cave crickets from Peloponnese (Orthoptera, Rhaphidophoridae): molecular and morphological investigations reveal four new species for Greece. *European Zoological Journal*, 88, 505–524. Available from: https://doi.org/10.1080/24750263.2021.1902005

Anderson, M.J. (2001) A new method for non-parametric multivariate analysis of variance. *Austral Ecology*, 26, 32–46. Available from: https://doi.org/10.1111/j.1442-9993.2001.01070.pp.x

April, J., Hanner, R.H., Dion-Côté, A.M. & Bernatchez, L. (2013) Glacial cycles as an allopatric speciation pump in north-eastern American freshwater fishes. *Molecular Ecology*, 22(2), 409–422. Available from: https://doi.org/10.1111/mec.12116

Barton, N.H. & Hewitt, G.M. (1985) Analysis of hybrid zones. *Annual Review of Ecology and Systematics*, 16, 113–148.

Bennett, K.D. & Provan, J. (2008) What do we mean by refugia? *Quaternary Science Reviews*, 27(27–28), 2449–2455. Available from: https://doi.org/10.1016/j.quascirev.2008.08.019

Bickford, D., Lohman, D.J., Sodhi, N.S., Ng, P.K.L., Meier, R., Winker, K. et al. (2007) Cryptic species as a window on diversity and conservation. *Trends in Ecology & Evolution*, 22(3), 148–155. Available from: https://doi.org/10.1016/j.tree.2006.11.004

Carstens, B.C. & Knowles, L.L. (2007) Shifting distributions and speciation: species divergence during rapid climate change. *Molecular Ecology*, 16(3), 619–627. Available from: https://doi.org/10.1080/10635150701405560

Chan, K.O., Mulcahy, D.G. & Anuar, S. (2023) The artefactual branch effect and phylogenetic conflict: species delimitation with gene flow in mangrove pit vipers (*Trimeresurus purpureomaculatus-erythrurus* Complex). *Systematic Biology*, 72(6), 1209–1219. Available from: https://doi.org/10.1093/sysbio/syad043

Chapco, W. & Litzenberger, G. (2002) A molecular phylogenetic study of two relict species of melanopline grasshoppers. *Genome*, 45(2), 313–318. Available from: https://doi.org/10.1139/g01-156

Cigliano, M.M., Braun, H., Eades, D.C. & Otte, D. (2025) *Orthoptera species file (OSF)*. Available from: http://orthoptera.speciesfile.org

Collier, R.E.L. & Dart, C.J. (1991) Neogene to quaternary rifting, sedimentation and uplift in the Corinth Basin, Greece. *Journal of the Geological Society*, 148, 1049–1065. Available from: https://doi.org/10.1144/gsjgs.148.6.104

Collyer, M.L. & Adams, D.C. (2018) RRPP: an R package for fitting linear models to high-dimensional data using residual randomization. *Methods in Ecology and Evolution*, 9, 1772–1779. Available from: https://doi.org/10.1111/2041-210X.13029

Coyne, J.A. & Orr, H.A. (1989) Patterns of speciation in *Drosophila*. *Evolution*, 43, 362–381.

Coyne, J.A. & Orr, H.A. (2004) *Speciation*. Sunderland, MA: Sinauer Associates.

De Queiroz, K. (2007) Species concepts and species delimitation. *Systematic Biology*, 56(6), 879–886. Available from: https://doi.org/10.1080/10635150701701083

Degnan, J.H. & Rosenberg, N.A. (2009) Gene tree discordance, phylogenetic inference and the multispecies coalescent. *Trends in Ecology & Evolution*, 24(6), 332–340. Available from: https://doi.org/10.1016/j.tree.2009.01.009

Durand, E.Y., Patterson, N., Reich, D. & Slatkin, M. (2011) Testing for ancient admixture between closely related populations. *Molecular Biology and Evolution*, 28(8), 2239–2252. Available from: https://doi.org/10.1093/molbev/msr048

Dussex, N., Chuah, A. & Waters, J.M. (2016) Genome-wide SNPs reveal fine-scale differentiation among wingless alpine stonefly populations and introgression between winged and wingless forms. *Evolution*, 70, 38–47. Available from: https://doi.org/10.1111/evo.12826

Dynesius, M. & Jansson, R. (2014) Persistence of within-species lineages: a neglected control of speciation rates. *Evolution*, 68(4), 923–934. Available from: https://doi.org/10.1111/evo.12316

Earl, D.A. & vonHoldt, B.M. (2012) STRUCTURE HARVESTER: a website and program for visualizing structure output and implementing the evanno method. *Conservation Genetics Resources*, 4, 359–361. Available from: https://doi.org/10.1007/s12686-011-9548-7

Eaton, D.A.R. & Overcast, I. (2020) IPYRAD: interactive assembly and analysis of RADseq datasets. *Bioinformatics*, 3(8), 2592–2594. Available from: https://doi.org/10.1093/bioinformatics/btz966

Ebdon, S., Laetsch, D.R., Dapporto, L., Hayward, A., Ritchie, M.G., Dincă, V. et al. (2021) The Pleistocene species pump past its prime: evidence from European butterfly sister species. *Molecular Ecology*, 30(14), 3575–3589. Available from: https://doi.org/10.1111/mec.15981

Evanno, G., Regnaut, S. & Goudet, J. (2005) Detecting the number of clusters of individuals using the software STRUCTURE: a simulation study. *Molecular Ecology*, 14(8), 2611–2620. Available from: https://doi.org/10.1111/j.1365-294X.2005.02553.x

Excoffier, L., Marchi, N., Marques, D.A., Matthey-Doret, R., Gouy, A. & Sousa, V.C. (2021) FASTSIMCOAL2: demographic inference under complex evolutionary scenarios. *Bioinformatics*, 37, 4882–4885. Available from: https://doi.org/10.1093/bioinformatics/btab468

Flouri, T., Jiao, X.Y., Rannala, B. & Yang, Z.H. (2018) Species tree inference with BPP using genomic sequences and the multispecies coalescent. *Molecular Biology and Evolution*, 35(10), 2585–2593. Available from: https://doi.org/10.1093/molbev/msy147

Funk, S.M., Guedaoura, S., Juras, R., Raziq, A., Landolsi, F., Luís, C. et al. (2020) Major inconsistencies of inferred population genetic structure estimated in a large set of domestic horse breeds using microsatellites. *Ecology and Evolution*, 10, 4261–4279. Available from: https://doi.org/10.1002/ece3.6195

García-Navas, V., Noguerales, V., Cordero, P.J. & Ortego, J. (2017a) Phenotypic disparity in Iberian short-horned grasshoppers (Acrididae): the role of ecology and phylogeny. *BMC Ecology and Evolution*, 17, 109. Available from: https://doi.org/10.1186/s12862-017-0954-7

García-Navas, V., Noguerales, V., Cordero, P.J. & Ortego, J. (2017b) Ecological drivers of body size evolution and sexual size dimorphism in short-horned grasshoppers (Orthoptera: Acrididae). *Journal of Evolutionary Biology*, 30, 1592–1608. Available from: https://doi.org/10.1111/jeb.13131

Gilbert, K.J., Andrew, R.L., Bock, D.G., Franklin, M.T., Kane, N.C., Moore, J.S. et al. (2012) Recommendations for utilizing and reporting population genetic analyses: the reproducibility of genetic clustering using the program STRUCTURE. *Molecular Ecology*, 21(20), 4925–4930. Available from: https://doi.org/10.1111/j.1365-294x.2012.05754.x

Haffer, J. (1969) Speciation in amazonian Forest birds. *Science*, 165(3889), 131–137. Available from: https://doi.org/10.1126/science.165.3889.131

Harrison, R.G. (1980) Dispersal polymorphisms in insects. *Annual Review of Ecology and Systematics*, 11, 95–118. Available from: https://doi.org/10.1146/annurev.es.11.110180.000523

Harrison, R.G. & Larson, E.L. (2014) Hybridization, introgression, and the nature of species boundaries. *Journal of Heredity*, 105, 795–809. Available from: https://doi.org/10.1093/jhered/esu033

Hawlitschek, O., Ortiz, E.M., Noori, S., Webster, K.C., Husemann, M. & Pereira, R.J. (2022) Transcriptomic data reveals nuclear-mitochondrial discordance in Gomphocerinae grasshoppers (Insecta: Orthoptera: Acrididae). *Molecular Phylogenetics and Evolution*, 170, 107439. Available from: https://doi.org/10.1016/j.ympev.2022.107439

Hewitt, G.M. (1996) Some genetic consequences of ice ages, and their role in divergence and speciation. *Biological Journal of the Linnean Society*, 58(3), 247–276. Available from: https://doi.org/10.1006/bijl.1996.0035

Hewitt, G.M. (2000) The genetic legacy of the Quaternary ice ages. *Nature*, 405(6789), 907–913. Available from: https://doi.org/10.1038/35016000

Hochkirch, A. & Damerau, M. (2009) Rapid range expansion of a wing dimorphic bush-cricket after the 2003 climatic anomaly. *Biological Journal of the Linnean Society*, 97, 118–127. Available from: https://doi.org/10.1111/j.1095-8312.2008.01199.x

Hochkirch, A., Nieto, A., García Criado, M., Cálix, M., Braud, Y., Buzzetti, F.M. et al. (2016) *European red list of grasshoppers, crickets and bush-crickets*. Luxembourg: Publications Office of the European Union. Available from: https://doi.org/10.2779/60944

Huang, J.P. (2016) Parapatric genetic introgression and phenotypic assimilation: testing conditions for introgression between Hercules beetles (*Dynastes*, Dynastinae). *Molecular Ecology*, 25(21), 5513–5526. Available from: https://doi.org/10.1111/mec.13849

Huang, J.P., Hill, J.G., Ortego, J. & Knowles, L.L. (2020) Paraphyletic species no more—genomic data resolve a Pleistocene radiation and validate morphological species of the *Melanoplus scudderi* complex (Insecta: Orthoptera). *Systematic Entomology*, 45, 594–605. Available from: https://doi.org/10.1111/syen.12415

Hughes, P.D., Woodward, J.C. & Gibbard, P.L. (2006) Quaternary glacial history of the Mediterranean mountains. *Progress in Physical Geography*, 30(3), 334–364. Available from: https://doi.org/10.1191/0309133306pp481ra

Ikeda, H., Nishikawa, M. & Sota, T. (2012) Loss of flight promotes beetle diversification. *Nature Communications*, 3, 648. Available from: https://doi.org/10.1038/ncomms1659

Jakobsson, M. & Rosenberg, N.A. (2007) CLUMPP: a cluster matching and permutation program for dealing with label switching and multimodality in analysis of population structure. *Bioinformatics*, 23, 1801–1806. Available from: https://doi.org/10.1093/bioinformatics/btm233

Janes, J.K., Miller, J.M., Dupuis, J.R., Malenfant, R.M., Gorrell, J.C., Cullingham, C.I. et al. (2017) The $K=2$ conundrum. *Molecular Ecology*, 26(14), 3594–3602. Available from: https://doi.org/10.1111/mec.14187

Kalinowski, S.T. (2011) The computer program STRUCTURE does not reliably identify the main genetic clusters within species: simulations and implications for human population structure. *Heredity*, 106, 625–632. Available from: https://doi.org/10.1038/hdy.2010.95

Keightley, P.D., Ness, R.W., Halligan, D.L. & Haddrill, P.R. (2014) Estimation of the spontaneous mutation rate per nucleotide site in a *Drosophila melanogaster* full-sib family. *Genetics*, 196(1), 313–320. Available from: https://doi.org/10.1534/genetics.113.158758

Keightley, P.D., Pinharanda, A., Ness, R.W., Simpson, F., Dasmahapatra, K.K., Mallet, J. et al. (2015) Estimation of the spontaneous mutation rate in *Heliconius melpomene*. *Molecular Biology and Evolution*, 32(1), 239–243. Available from: https://doi.org/10.1093/molbev/msu302

Kiourtsoglou, A., Kaliontzopoulou, A., Poursanidis, D., Jablonsky, D., Lymberakis, P. & Poulakakis, N. (2021) Evidence of cryptic diversity in *Podarcis peloponnesiacus* and re-evaluation of its current taxonomy; insights from genetic, morphological, and ecological data. *Journal of Zoological Systematics and Evolutionary Research*, 59(8), 2350–2370. Available from: https://doi.org/10.1111/jzs.12540

Knowles, L.L. & Massatti, R. (2017) Distributional shifts – not geographical isolation – As a probable driver of montane species divergence. *Ecography*, 40(12), 1475–1485. Available from: https://doi.org/10.1111/ecog.02893

Le Flanchec, T., Robillard, T., Hill, J.G., Hemp, C. & Nattier, R. (2026) Inverse latitudinal diversity gradient, systematics and historical biogeography in the Gomphocerinae grasshoppers (Orthoptera: Acrididae). *Zoologica Scripta*, 55(1), 102–115. Available from: https://doi.org/10.1111/zsc.70014

Lewis, P.O. (2001) A likelihood approach to estimating phylogeny from discrete morphologicalcharacter data. *Systematic Biology*, 50(6), 913–925. Available from: https://doi.org/10.1080/10635150175346287 6

Maddison, W.P. & Knowles, L.L. (2006) Inferring phylogeny despite incomplete lineage sorting. *Systematic Biology*, 55(1), 21–30. Available from: https://doi.org/10.1080/10635150500354928

Maier, P.A., Vandergast, A.G., Ostoja, S.M., Aguilar, A. & Bohonak, A.J. (2019) Pleistocene glacial cycles drove lineage diversification and fusion in the Yosemite toad (*Anaxyrus canorus*). *Evolution*, 73(12), 2476–2496. Available from: https://doi.org/10.1111/evo.13868

Mallet, J., Besansky, N. & Hahn, M.W. (2016) How reticulated are species? *BioEssays*, 38(2), 140–149. Available from: https://doi.org/10.1002/bies.201500149

Mason, P.L., Nichols, R.A. & Hewitt, G.M. (1995) Philopatry in the alpine grasshopper, *Podisma pedestris*: a novel experimental and analytical method. *Ecological Entomology*, 20(2), 137–145. Available from: https://doi.org/10.1111/j.1365-2311.1995.tb00439.x

Mayr, E. (1963) *Animal species and evolution*. Cambridge: Belknap Press of Harvard University Press.

McCulloch, G.A., Foster, B.J., Dutoit, L. & Waters, J.M. (2022) Repeated Alpine flight loss within the widespread New Zealand stonefly *Nesoperla fulvescens* hare (Plecoptera: Gripopterygidae). *Insect Systematics and Diversity*, 6(6), 1–9. Available from: https://doi.org/10.1093/isd/ixac027

Myers, N., Mittermeier, R.A., Mittermeier, C.G., da Fonseca, G.A.B. & Kent, J. (2000) Biodiversity hotspots for conservation priorities. *Nature*, 403(6772), 853–858. Available from: https://doi.org/10.1038/35002501

Neumeister, D.S., González-Ramírez, D.C., Gaugel, S.M., Yazici, T.D., Haug, J.T., Schielzeth, H. et al. (2025) Clarifying diversity in the radiation of *Chorthippus* grasshoppers (Orthoptera: Acrididae) through an integration of genomic and morphometric approaches. *Zoological Journal of the Linnean Society*, 204(4), zlaf076. Available from: https://doi.org/10.1093/zoolinnean/zlaf076

Nevado, B., Contreras-Ortiz, N., Hughes, C. & Filatov, D.A. (2018) Pleistocene glacial cycles drive isolation, gene flow and speciation in the high-elevation Andes. *New Phytologist*, 219(2), 779–793. Available from: https://doi.org/10.1111/nph.15243

Nieto-Feliner, G. (2011) Southern European glacial refugia: a tale of tales. *Taxon*, 60(2), 365–372. Available from: https://doi.org/10.1002/tax.602007

Noguerales, V., Cordero, P.J. & Ortego, J. (2018) Integrating genomic and phenotypic data to evaluate alternative phylogenetic and species delimitation hypotheses in a recent evolutionary radiation of grasshoppers. *Molecular Ecology*, 27(5), 1229–1244. Available from: https://doi.org/10.1111/mec.14504

Noguerales, V. & Ortego, J. (2022) Genomic evidence of speciation by fusion in a recent radiation of grasshoppers. *Evolution*, 76(11), 2618–2633. Available from: https://doi.org/10.1111/evo.14508

Nosil, P. (2008) Speciation with gene flow could be common. *Molecular Ecology*, 17(9), 2103–2106. Available from: https://doi.org/10.1111/j.1365-294x.2008.03715.x

Olsen, A.M. & Westneat, M.W. (2015) StereoMorph: An R package for the collection of 3D landmarks and curves using a stereo camera setup. *Methods in Ecology and Evolution*, 6(3), 351–356. Available from: https://doi.org/10.1111/2041-210X.12326

Ortego, J., Aguirre, M.P. & Cordero, P.J. (2012) Genetic and morphological divergence at different spatiotemporal scales in the grasshopper *Mioscirtus wagneri* (Orthoptera: Acrididae). *Journal of Insect Conservation*, 16, 103–110. Available from: https://doi.org/10.1007/s10841-011-9397-4

Ortego, J., Gutiérrez-Rodríguez, J. & Noguerales, V. (2021) Demographic consequences of dispersal-related trait shift in two recently diverged taxa of montane grasshoppers. *Evolution*, 75(8), 1998–2013. Available from: https://doi.org/10.1111/evo.14205

Ortego, J., Kaya, S., Çiplak, B. & Knowles, L.L. (2024) Microgeographic speciation in a complex of Anatolian bush crickets facilitated by fast evolution of reproductive isolation. *Journal of Evolutionary Biology*, 37, 14–27. Available from: https://doi.org/10.1093/jeb/voad008

Ortego, J. & Knowles, L.L. (2022) Geographical isolation versus dispersal: Relictual alpine grasshoppers support a model of interglacial diversification with limited hybridization. *Molecular Ecology*, 31, 296–312. Available from: https://doi.org/10.1111/mec.16225

Ortego, J. & Noguerales, V. (2025) Mountain speciation driven by high rates of lineage formation and rapid evolution of partial reproductive isolation: insights from a recent radiation of grasshoppers (Orthoptera: Gomphocerinae). *Zoological Journal of the Linnean Society*, 205(2), zlaf141. Available from: https://doi.org/10.1093/zoolinnean/zlaf141

Ortego, J. & Trillo, M. (2026) Genomic-based species delimitation reveals cryptic diversity and semi-permeable species boundaries in a *Chorthippus* (Orthoptera: Acrididae) grasshopper complex from Greece. Figshare; Version 2. Dataset. Available from: https://doi.org/10.6084/m9.figshare.31136593

Ortego, J., Trillo, M., Gutiérrez-Rodríguez, J. & García-Navas, V. (2026) Latitudinal clines in gene flow and demographic stability reveal drivers of microendemism in a radiation of alpine grasshoppers. *Molecular Ecology*, 35(7), e70332. Available from: https://doi.org/10.1111/mec.70332

Payseur, B.A. & Rieseberg, L.H. (2016) A genomic perspective on hybridization and speciation. *Molecular Ecology*, 25(11), 2337–2360. Available from: https://doi.org/10.1111/mec.13557

Peterson, B.K., Weber, J.N., Kay, E.H., Fisher, H.S. & Hoekstra, H.E. (2012) Double digest RADseq: an inexpensive method for de novo SNP discovery and genotyping in model and non-model species. *PLoS One*, 7(5), e37135. Available from: https://doi.org/10.1371/journal.pone.0037135

Pritchard, J.K., Stephens, M. & Donnelly, P. (2000) Inference of population structure using multilocus genotype data. *Genetics*, 155(2), 945–959. Available from: https://doi.org/10.1093/genetics/155.2.945

Puechmaille, S.J. (2016) The program STRUCTURE does not reliably recover the correct population structure when sampling is uneven: subsampling and new estimators alleviate the problem. *Molecular Ecology Resources*, 16, 608–627. Available from: https://doi.org/10.1111/1755-0998.12512

R Core Team. (2021) *R: a language and environment for statistical computing*. Vienna, Austria: R Foundation for Statistical Computing. Available from: https://www.R-project.org/

Ramme, W. (1926) Neue und wenig bekannte europäische und asiatische Orthopteren (Acrid., Tettigon.). *Deutsche Entomologische Zeitschrift*, 4, 273–289.

Ramme, W. (1927) Die Dermapteren und Orthopteren Siziliens und Kretas. *Eos*, 3, 111–200.

Rannala, B. & Yang, Z. (2003) Bayes estimation of species divergence times and ancestral population sizes using DNA sequences from multiple loci. *Genetics*, 164, 1645–1656. Available from: https://doi.org/10.1093/genetics/164.4.1645

Rheindt, F.E., Fujita, M.K., Wilton, P.R. & Edwards, S. (2014) Introgression and phenotypic assimilation in *Zimmerius* flycatchers (Tyrannidae): population genetic and phylogenetic inferences from genome-wide SNPs. *Systematic Biology*, 63(2), 134–152. Available from: https://doi.org/10.1093/sysbio/syt070

Rochette, N.C., Rivera-Colón, A.G. & Catchen, J.M. (2019) STACKS 2: analytical methods for paired-end sequencing improve RADseq-based population genomics. *Molecular Ecology*, 28, 4737–4754. Available from: https://doi.org/10.1111/mec.15253

Roff, D.A. (1990) The evolution of flightlessness in insects. *Ecological Monographs*, 60, 389–421. Available from: https://doi.org/10.2307/1943013

Roff, D.A. (1994) Habitat persistence and the evolution of wing dimorphism in insects. *The American Naturalist*, 144(5), 772–798. Available from: https://doi.org/10.1086/285706

Rohlf, F.J. (1998) On applications of geometric morphometrics to studies of ontogeny and phylogeny. *Systematic Biology*, 47(1), 147–158. Available from: https://doi.org/10.1080/106351598261094

Rosenberg, N.A. (2004) DISTRUCT: a program for the graphical display of population structure. *Molecular Ecology Notes*, 4, 137–138. Available from: https://doi.org/10.1046/j.1471-8286.2003.00566.x

Schmidt, R., Dufresnes, C., Kristín, A., Künzel, S., Vences, M. & Hawlitschek, O. (2024) Phylogenetic insights into Central European *Chorthippus* and *Pseudochorthippus* (Orthoptera: Acrididae) species using ddRADseq data. *Molecular Phylogenetics and Evolution*, 193, 108012. Available from: https://doi.org/10.1016/j.ympev.2024.108012

Seehausen, O. (2004) Hybridization and adaptive radiation. *Trends in Ecology & Evolution*, 19(4), 198–207. Available from: https://doi.org/10.1016/j.tree.2004.01.003

Stamatakis, A. (2014) RAXML version 8: a tool for phylogenetic analysis and post-analysis of large phylogenies. *Bioinformatics*, 30, 1312–1313. Available from: https://doi.org/10.1093/bioinformatics/btu033

Stewart, J.R., Lister, A.M., Barnes, I. & Dalen, L. (2010) Refugia revisited: individualistic responses of species in space and time. *Proceedings of the Royal Society B*, 277, 661–671. Available from: https://doi.org/10.1098/rspb.2009.1272

Suárez, D., Arribas, P., Jiménez-García, E. & Brent, E.C. (2022) Dispersal ability and its consequences for population genetic differentiation and diversification. *Proceedings of the Royal Society B*, 289, 20220489. Available from: https://doi.org/10.1098/rspb.2022.0489

Sukumaran, J., Holder, M.T. & Knowles, L.L. (2021) Incorporating the speciation process into species delimitation. *PLoS Computational Biology*, 17(5), e1008924. Available from: https://doi.org/10.1371/journal.pcbi.1008924

Suzuki, T., Suzuki, N. & Tojo, K. (2019) Parallel evolution of an alpine type ecomorph in a scorpionfly: independent adaptation to high-altitude environments in multiple mountain locations. *Molecular Ecology*, 28(13), 3225–3240. Available from: https://doi.org/10.1111/mec.15119

Thanou, E., Jablonski, D. & Kornilios, P. (2023) Genome-wide single nucleotide polymorphisms reveal recurrent waves of speciation in niche-pockets, in Europe's most venomous snake. *Molecular Ecology*, 32(13), 3624–3640. Available from: https://doi.org/10.1111/mec.16944

Tonzo, V. & Ortego, J. (2021) Glacial connectivity and current population fragmentation in sky islands explain the contemporary distribution of genomic variation in two narrow-endemic montane grasshoppers from a biodiversity hotspot. *Diversity and Distributions*, 27(9), 1619–1633. Available from: https://doi.org/10.1111/ddi.13306

Tzortzakaki, O., Willemse, L.P.M. & Hochkirch, A. (2023a) *Chorthippus pulloides*. The IUCN red list of threatened species 2023: e.T16084479A226343370. Available from: https://doi.org/10.2305/IUCN.UK.2023-1.RLTS.T16084479A226343370.en [Accessed 30th August 2025].

Tzortzakaki, O., Willemse, L.P.M. & Hochkirch, A. (2023b) *Chorthippus parnon*. The IUCN red list of threatened species 2023: e.T16084456A226343243. Available from: https://doi.org/10.2305/IUCN.UK.2023-1.RLTS.T16084456A226343243.en [Accessed 30th August 2025].

Tzortzakaki, O., Willemse, L.P.M. & Hochkirch, A. (2023c) *Chorthippus crassiceps*. The IUCN red list of threatened species 2023: e.T16084613A226342815. Available from: https://doi.org/10.2305/IUCN.UK.2023-1.RLTS.T16084613A226342815.en [Accessed 30th August 2025].

Vedenina, V., Sevastianov, N. & Kovalyova, E. (2024) New data on bioacoustics and courtship behaviour in grasshoppers (Orthoptera, Acrididae, Gomphocerinae) from Russia and adjacent countries. *Zookeys*, 1200, 1–26. Available from: https://doi.org/10.3897/zookeys.1200.118422

Walsh, B. (2001) Estimating the time to the most recent common ancestor for the Y chromosome or mitochondrial DNA for a pair of individuals. *Genetics*, 158(2), 897–912. Available from: https://doi.org/10.1093/genetics/158.2.897

Willemse, F. (1984) Catalogue of the Orthoptera of Greece. *Fauna Graeciae*, 1, 1–275.

Willemse, F. (1985) Supplementary notes on the Orthoptera of Greece. *Fauna Graeciae*, 1ª, 1–47.

Willemse, F. (1986) A key to the Orthoptera species of Greece. *Fauna Graeciae*, 2, 1–288.

Willemse, F.M.H., von Helversen, O. & Odé, B. (2009) A review of *Chorthippus* species with angled pronotal lateral keels from Greece with special reference to transitional populations between some Peloponnesean taxa (Orthoptera, Acrididae). *Zoologische Mededelingen Leiden*, 83(2), 319–507.

Wright, N.A., Steadman, D.W. & Witt, C.C. (2016) Predictable evolution toward flightlessness in volant Island birds. *Proceedings of the National Academy of Sciences of the United States of America*, 113, 4765–4770. Available from: https://doi.org/10.1073/pnas.1522931113

Zera, A.J. & Denno, R.F. (1997) Physiology and ecology of dispersal polymorphism in insects. *Annual Review of Entomology*, 42, 207–230. Available from: https://doi.org/10.1146/annurev.ento.42.1.207

SUPPORTING INFORMATION

Additional supporting information can be found online in the Supporting Information section at the end of this article.

Methods S1. Genomic library preparation.

Methods S2. Genomic data filtering and assembling.

Methods S3 FASTSIMCOAL2 analyses and model selection.

Table S1. Description and numbering of landmarks used for geometric morphometric analyses of (A) forewing and (B) pronotum-head combined (depicted in Figure 1).

Table S2. Attributes of genomic datasets used for different analyses, including number of individuals in the ingroup/outgroup and number of retained reads and loci after different filtering steps in STACKS and IPYRAD.

Table S3. Analyses of introgression based on four-taxon *D*-statistic (ABBA/BABA) tests. Analyses were designed to test for introgression from one taxon (P3) into each genotyped individual of the focal population (P1). For both P2 and P3, we used reference populations with no signatures of genetic introgression from other taxa. The highly divergent lineage from Mt. Kakarditsa (KAKA) was used as an outgroup (P4) in all analyses. Population codes as described in Table 1.

Table S4. Pairwise Procrustes distances (*d*) among populations of the *Chorthippus* species complex in Greece based on male forewing shape variation. Values in bold indicate statistically significant Procrustes distances after false discovery rate adjustment (FDR) to control for multiple tests (FDR of 5%, $q < 0.05$). Due to small sample sizes, statistical significance was not assessed for pairwise comparisons involving populations KRIO and STEM (Table 1). Population codes as described in Table 1.

Table S5. Pairwise Procrustes distances (*d*) among populations of the *Chorthippus* species complex in Greece based on male pronotum-head shape variation. Values in bold indicate statistically significant Procrustes distances after false discovery rate adjustment (FDR) to control for multiple tests (FDR of 5%, $q < 0.05$). Due to small sample sizes, statistical significance was not assessed for pairwise comparisons involving populations KRIO and STEM (Table 1). Population codes as described in Table 1.

Table S6. Pairwise Procrustes distances (*d*) among delineated species within the *Chorthippus* species complex in Greece based on male forewing shape variation. Statistically significant values after false discovery rate adjustment (FDR) to control for multiple tests (FDR of 5%, $q < 0.05$) are indicated in bold. Population codes for the three populations (KAKA, AKAR and POTA) that were delineated as new species correspond to those presented in Table 1.

Table S7. Pairwise Procrustes distances (*d*) among delineated species within the *Chorthippus* species complex in Greece based on male pronotum-head shape variation. Statistically significant values after false discovery rate adjustment (FDR) to control for multiple tests (FDR of 5%, $q < 0.05$) are indicated in bold. Population codes for the three populations (KAKA, AKAR and POTA) that were delineated as new species correspond to those presented in Table 1.

Table S8. Post hoc Tukey's tests for differences in forewing-to-femur length ratio (TL/FL) of males among populations of the *Chorthippus* species complex in Greece. Adjusted *p*-values are reported, with values in bold indicating significant comparisons. Due to small sample sizes, statistical significance was not assessed for pairwise comparisons involving these populations KRIO and STEM (Table 1). Population codes as described in Table 1.

Table S9 Post hoc Tukey's tests for differences in forewing-to-femur length ratio (FWL/FL) of males among delineated species within the *Chorthippus* species complex in Greece. Adjusted *p*-values are reported, with values in bold indicating significant comparisons. Population codes for the three populations (KAKA, AKAR and POTA) that were delineated as new species correspond to those presented in Table 1.

Figure S1. Alternative models of divergence and admixture tested using FASTSIMCOAL2 for three population triplets including hybrid populations (MAEN, PARN, TAYP) and representative populations of their parental taxa *C. pulloides* (KYLL) and *C. moreanus* (PYLO, TENA) or *C. parnon* (MALE). Population codes as described in Table 1. Models include scenarios of divergence in strict isolation followed by an admixture event

and interruption of contemporary gene flow (Model A), and divergence in strict isolation followed by an admixture event and contemporary gene flow (Model B). Parameters include mutation-scaled ancestral and contemporary effective population sizes (θ), the proportion of lineages inherited from *C. pulloides* (r), migration rates per generation (m) and timing of divergence (T_{DIV}) and admixture (T_{ADMIX}).

Figure S2. Phylogenetic tree inferred with RAXML and divergence times estimated using BPP (analysis A00) for the analyzed populations of the *Chorthippus* species complex in Greece. Admixed populations identified by STRUCTURE for $K = 6$ (marked with an asterisk in Figure 3b) were excluded from phylogenomic analyses (see Testing for introgression and Population genetic structure). Bootstrap support values estimated with RAXML are indicated at nodes (*>95%). Bars on nodes indicate 95% highest posterior densities (HPD) of divergence times estimated considering a genomic mutation rate of 2.8×10^{-9} per site per generation and a one-year generation time. Branch colours correspond to the predominant genetic cluster to which each population was assigned based on STRUCTURE analyses for $K = 6$ (see Figure 3b) and background colours indicate geological divisions of the Quaternary. The taxonomic status of populations before (input;? = unknown) and after (output) species delimitation analyses in DELINEATE is shown on the right; DELINEATE uses the ultrametric phylogeny inferred with BPP together with prior species assignments for a subset of populations (input) to evaluate whether the remaining populations belong to previously described species or represent distinct lineages. Population codes as described in Table 1. The inset image shows a male of the short-winged *C. pulloides* (illustration by Marina Trillo).

Figure S3. Phylogenetic tree inferred with RAXML including all sampled populations (i.e., without excluding admixed populations) of the *Chorthippus* species complex in Greece. Bootstrap support values estimated with RAXML are indicated at nodes (*>95%). Branch colours correspond to the predominant genetic cluster to which each population was assigned based on STRUCTURE analyses for $K = 6$ (see Figure 3b); admixed populations are shown in grey. Newly delimited species identified with DELINEATE are labelled as 'DelineatedSp'. Population codes as described in Table 1.

Figure S4. Results of STRUCTURE for analyzed populations of the *Chorthippus* species complex in Greece distributed within the Peloponnese Peninsula. Panels show mean (±SD) log probability of the data (LnPr(X|K)) over 10 runs of STRUCTURE (left axes, black dots and error bars) for each value of K and the magnitude of ΔK (right axes, blue triangles).

Figure S5. Results of genetic assignments based on the program STRUCTURE (5426 SNPs) for analyzed populations of the *Chorthippus* species complex in Greece distributed within the Peloponnese Peninsula. Each individual is represented by a vertical bar partitioned into K coloured segments showing the individual's probability of belonging to the cluster with that colour; thin vertical black lines separate individuals from different populations. Population codes as described in Table 1.

Figure S6. Principal component analyses of male forewing shape variation across studied populations of the *Chorthippus* species complex in Greece based on (A) raw and (B) size-corrected Procrustes coordinates. Populations are coloured according to their corresponding lineages in the phylogenetic tree (Figure 2) and the main genetic cluster to which genetically admixed populations (marked with an asterisk) were assigned based on STRUCTURE analyses (Figure 3). Population codes as described in Table 1.

Figure S7. Principal component analyses of male pronotum-head shape variation across studied populations of the *Chorthippus* species complex in Greece based on (A) raw (A) and (B) size-corrected Procrustes coordinates. Populations are coloured according to their corresponding lineages in the phylogenetic tree (Figure 2) and the main genetic cluster to which genetically admixed populations (marked with an asterisk) were assigned based on STRUCTURE analyses (Figure 3). Population codes as described in Table 1.

How to cite this article: Trillo, M. & Ortego, J. (2026) Genomic-based species delimitation reveals cryptic diversity and semi-permeable species boundaries in a *Chorthippus* (Orthoptera: Acrididae) grasshopper complex from Greece. *Systematic Entomology*, 51(2), e70051. Available from: https://doi.org/10.1111/syen.70051